

1 Larval dispersal of intertidal organisms  
2 and the influence of coastline  
3 geography

---

4

5 Thomas P. Adams\*

6 Dmitry Aleynik

7 Michael T. Burrows

8

9 Scottish Association for Marine Science, Scottish Marine Institute, Dunbeg, Oban, PA37 1QA, UK

10 \* Corresponding author: [tom.adams@sams.ac.uk](mailto:tom.adams@sams.ac.uk)

11

12

13 Running head: Larval dispersal and coastal geography

14

15 Keywords: Connectivity, larval dispersal, intertidal ecology, marine population, coastal geography

## 16 **Abstract**

17 The dispersal stages of organisms with sessile adults must be able to select habitats with suitable  
18 environmental conditions for establishment and survival, and also must be able to reach those  
19 locations. For marine planktonic larvae, movement due to currents is often orders of magnitude  
20 greater than movement due to swimming behaviour, so transport to adult habitats is largely passive.

21 Current patterns are determined by interactions between underlying geography and tidal forces,  
22 modified by meteorological conditions. These linkages impose an area-specific focus to connectivity  
23 studies. Yet, how geographical features and meteorological forcing combine to produce specific  
24 current patterns and resultant connectivity among populations remains unclear.

25 In this study of a complex fjordic region (the Firth of Lorn, Scotland), we followed tracks of generic  
26 particles driven by modelled hydrodynamic currents to investigate how connectivity between evenly  
27 spaced habitat sites varies in relation to coastal topography. We studied a range of larval durations  
28 (1-28 days), and two different but typical meteorological forcing scenarios. Particles released from  
29 regions of high current velocity, open coastline and low local habitat availability travelled furthest  
30 but were less likely to disperse successfully to other coastal sites. Extensive natal habitat in the  
31 vicinity of a site generally had a positive impact on the number of arriving particles, as did low  
32 current velocities. However, relationships between numbers of arriving particles and local  
33 geographical indices were complex, particularly at longer larval durations.

34 Local geography alone explained up to 50% of the variance in success of particles released and closer  
35 to 10% of the variation in the number of particles arriving at each site. General patterns are evident,  
36 but coastline properties fall short of predicting dispersal measures for particular locations. The study  
37 shows that meteorological variation and broad scale current patterns interact strongly with local  
38 geography to determine connectivity in coastal areas.

## 39 **1 INTRODUCTION**

40 Understanding the structure and dynamics of biological populations is a central aim of ecology. In  
41 the case of marine organisms, a feature uniting diverse taxa has been the evolution of a life cycle  
42 entailing two- (or more) stages; a sessile adult stage, and a pelagic larval stage (Pineda et al. 2007).  
43 Population structure therefore depends on a wide range of factors, and populations may be limited  
44 by space (competition, or lack of space for new settlers; Roughgarden et al. 1985), environmental  
45 conditions (that determine food uptake, rates of growth, survival and reproduction  
46 (Brown 1984, Burrows et al. 2010) or recruitment (where there is insufficient larval supply to  
47 saturate available habitat; Jenkins et al. 2008). However, larvae may settle great distances from their  
48 parent populations (Gaines et al. 2007), meaning that reproduction and recruitment at a given  
49 location are disconnected.

50 Early studies of marine organisms with pelagic dispersal considered the “larval pool”: a  
51 homogeneous and supply of larvae that settle into the adult population (Roughgarden et al. 1985,  
52 Moko and Iwasa 2000). However, pelagic larvae move primarily according to local hydrodynamics.  
53 Studies investigating the impact of basic hydrodynamic effects have linked spatial and temporal  
54 variations in larval abundance in the ocean to features such as currents, fronts, and coastal  
55 boundary layers (Largier 2003, Ayata et al. 2010, Robins et al. 2013). However, despite much work  
56 aiming to understand the driving forces on population dynamics of coastal intertidal organisms  
57 (including rates of larval settlement; Bertness et al. 1996; Hawkins and Hartnoll 1982), no systematic  
58 attempt has been made to link coastal geography with larval supply. This is partly due to the  
59 difficulties involved in collecting sufficient data along the entire coastline, but also due to  
60 complicating factors such as variability in meteorological conditions between sampling events, and  
61 their interactions with an inhomogeneous coastline.

62 Our inability to track larvae directly has meant that simulation modelling has always been a central  
63 component of the evaluation of larval dispersal and its impact on population dynamics. The early

64 model of Roughgarden et al. (1985) has been developed to include idealised representations of  
65 hydrodynamic forces (Possingham and Roughgarden 1990, Rio Doce et al. 2008). These models aim  
66 to capture whole life cycles over a timescale of years. In contrast, more detailed studies of larval  
67 dispersal tend to implement a timescale of seconds to hours, ultimately aiming to understand how  
68 movements affect larval abundance over a single dispersal period or season. While generally  
69 performed in isolation, these studies complement life cycle models by linking reproduction and  
70 recruitment rates of geographically separated sites.

71 Simulations of larval dispersal involve a coupling of hydrodynamic and biological models. Some  
72 studies have obtained general results used idealised hydrodynamics (Siegel et al. 2003, Gaines et al.  
73 2003), but most have used bespoke model implementations for particular regions of interest (e.g.  
74 Aiken et al. 2007, North et al. 2008, Mitarai et al. 2009). These allow representation of specific  
75 topography, freshwater influx, prevailing meteorological conditions and so on. Relevant boundary  
76 conditions for small scale models are generally derived from coarser models, which have been  
77 validated at larger scales over many years (e.g. Blumberg and Mellor 1987). Accurate modelling of  
78 coastal regions is more complex, and involves a balance between computational expense and spatial  
79 resolution. Finite element methods (computation using a variable resolution triangular grid, in  
80 contrast to a regular square grid) have recently brought dramatic increases in the spatial and  
81 temporal scope of models, providing both accuracy and efficiency (Zhao et al. 2006, Huang et al.  
82 2008) with representation of key topographical features over a very wide range of spatial scales  
83 (particularly important for complex coastal regions; Chen et al. 2003). We adopt this approach to  
84 hydrodynamic modelling here.

85 The representation of larval biology in transport models varies widely, and from general to highly  
86 species specific. In the simplest models larvae are considered as passive particles, with movement  
87 driven by advective and diffusive processes in the hydrodynamic model (e.g. Gaines et al. 2003). A  
88 degree of biological realism is often added by incorporating mortality, either at a constant (Trembl et

89 al. 2008, Adams et al. 2012) or environmentally dependent rate, and also via some form of  
90 development. Ontogenetic change in larval behaviour may entail a switch in ability to settle  
91 (Amundrud and Murray 2009), but may involve changes in swimming behaviour. Marine larvae show  
92 various swimming behaviours that may allow them to either resist or take advantage of water  
93 currents. The larvae of some coral-reef fish are known to actively locate their “home” reefs (Radford  
94 et al. 2011), while late-stage sea lice larvae swim towards potential hosts (summarised by Costello  
95 2009). Vertical migration may occur in response to light (for feeding or predator evasion, for  
96 example Dobretsov and Miron 2001), aversion to freshwater (Gillibrand and Willis 2007), or to aid  
97 location of suitable adult habitat (for example intertidal zonation; Grosberg 1982). Temporarily  
98 moving to the sea bed where currents are slower, or “selective tidal stream transport” (Crales et al.  
99 2011) also allows larvae to avoid flow in the opposite direction to that required to reach suitable  
100 habitat. For larvae aiming to reach inshore areas, such behaviour avoids the the ebbing tide (Knights  
101 et al. 2006, Fox et al. 2006, 2009, North et al. 2008), while for other species this can permit travel  
102 over much greater distances (Sundelöf and Jonsson 2011).

103 Despite the existence of many studies of the link between oceanography and dispersal, none have  
104 sought to systematically investigate how the geographical location of sources of larvae and sites for  
105 settlement affect potential dispersal and recruitment. Here we implement a combination of recently  
106 developed coastal hydrodynamic and particle tracking models in a region with high variability in  
107 coastal topography over small to medium scales. By considering release of particles (exhibiting  
108 either no behaviour or simple selective tidal stream behaviour) from evenly distributed habitat along  
109 the coastline, we aim to understand the role of specific sites in the regional population.

110 Specifically, we firstly ask what determines how far larvae travel from their parent habitat. Dispersal  
111 kernels are often estimated in terrestrial ecology (Kot et al., 1996) but more commonly take an  
112 assumed form in marine studies, based upon diffusion alone, homogeneous current speeds (Gaines  
113 et al. 2003), or probability inversely proportional to seaway distance (Kristoffersen et al. in press).

114 Aiken et al. (2007) found that spatially and temporally homogeneous estimates of dispersal were  
115 likely to be insufficient, even for a relatively homogeneous coastline. Secondly, we ask what makes a  
116 site an important “source” or “sink” for larvae. Finally, does pelagic larval duration alter the  
117 importance of site characteristics? In summary, we hope to determine whether geographical  
118 properties of coastal sites can be used to predict their hydrodynamic connectivity.

119 There are good reasons for making hypotheses about the likely relationships. Crisp et al. (1982)  
120 suggested that species with a long pelagic life might be suited to headlands, and those with short  
121 pelagic life to sheltered and embayed areas. Intuitively, open and exposed areas might lend  
122 themselves well to allowing long range dispersal, but also to a “dilution” of the dispersing larvae  
123 (and the possible failure of these larvae to reach suitable habitat). These same open areas may be  
124 exposed to large scale flow patterns, enhancing acquisition of larvae from other sources. The  
125 amount of nearby habitat is also likely to have an impact on the properties of a site. It might be  
126 expected that abundant nearby habitat might enhance supply directly. It might also alter local  
127 hydrodynamics in such a way that encourages retention, potentially increasing dispersal success and  
128 in particular self-recruitment. Aside from particular hydrodynamic features that enable retention to  
129 occur, local water velocity may also be of importance to dispersal. High velocities enable fast  
130 movement, logically suggesting long-range dispersal. However, it is not obvious whether this is likely  
131 to have an impact on the source/sink nature of coastal habitats. How these features combine to  
132 contribute to dispersal potential will be our core focus here.

## 133 **2 METHODS**

### 134 **2.1 Hydrodynamic model**

#### 135 **2.1.1 Unstructured model description**

136 This section provides a brief summary of the hydrodynamic model. Complete details are available in  
137 Appendix 1. Our hydrodynamic model was based on the unstructured grid Finite Volume Coastal

138 Ocean Model (FVCOM; Chen et al. 2003). Our implementation used 25071 triangular horizontal  
139 model elements and 11 terrain-following sigma-coordinates, allowing the geometric flexibility which  
140 is essential for fitting the irregular coastal geometry and bathymetry of south-west Scotland.  
141 Achieving a 100m minimum resolution in a regular lattice model (POLCOMS) of Loch Lihne (a small  
142 subset of our domain here) required a grid containing 365x488 elements (Ivanov et al. 2011); our  
143 model obtains improved maximum spatial resolution and increased domain size at lower  
144 computational expense. The mesh was refined over steep bathymetric features and around islands  
145 and narrow straits. Model bathymetry was based on a combination of the gridded SeaZone database  
146 (SeaZone 2007), high resolution Admiralty charts and side-sonar and multibeam surveys undertaken  
147 between 1999-2012 (J. Howe, unpublished data).

148 Horizontal diffusion in the model was based on the Smagorinsky (1963) eddy parameterisation, with  
149 mixing coefficient  $C=0.2$ . Vertical eddy diffusivity ( $K_m$ ) and vertical thermal diffusion ( $K_h$ ) were  
150 resolved with a Mellor-Yamada level 2.5 turbulence closure scheme (Mellor and Yamada, 1982). The  
151 model's bottom boundary layer was parameterised with a logarithmic wall-layer law. Since spatial  
152 variation of bottom roughness is not directly determined over the model domain, we chose to  
153 globally assign the minimal constant values for bottom drag coefficient as  $C_{d0}=0.0025$  and the  
154 roughness parameter as  $Z_0=0.003$ .

155 The model was solved numerically with a mode-split integration method. For stable operation with  
156 the selected mesh geometry (edge length 70-4650m), the upper bound of the external (barotropic)  
157 time step was  $\Delta T_E=0.47$  seconds. The actual value implemented was 0.4s, allowing for sporadic  
158 strong tunnelling winds. The internal (baroclinic) mode time step (4s) was  $\Delta T_I = I_{split} \Delta T_E$ , where  
159  $I_{split}=10$ . Model integration time (5 month run) was 24 hours, using 192 AMD Interlagos Opteron 2.3  
160 GHz processors at the HECToR centre.

161 **2.1.2 Model forcing**

162 The model's initial temperature and salinity field combined gridded data from the UK Hydrographic  
163 Office with local CTD data sets, and was resampled on the triangular mesh using a distance weighted  
164 algorithm (Barnes 1964). The model develops a full temperature and salinity adjustment to the  
165 tidally forced current field within a two week spin-up period.

166 Met-forcing included precipitation and evaporation rates, atmospheric pressure, wind speed and  
167 direction, short wave radiation and net heat flux. Hourly data from 5 coastal MetOffice weather  
168 stations in the region were interpolated over the model domain. Time series of discharge for 28  
169 main rivers were estimated from watershed areas (Edwards and Sharples 1986) and daily estimates  
170 of precipitation rate.

171 Boundary conditions for the hydrodynamic model were derived from the NE Atlantic Model  
172 developed by project partners in the EU ASIMUTH project at the Irish Marine Institute. Temperature  
173 and salinity were interpolated to the boundary nodes of our domain. Experiments indicated that  
174 spectral tidal constituents derived from the NW European shelf Tidal Data Inversion model (Egbert  
175 et al., 2010) improved model behaviour, and so these were used for all presented simulations.

176 **2.1.3 Model validation**

177 The model reproduced well-known patterns in the distribution of the 4 main tidal constituencies  
178 (M2, S2, K1 and O1), shown on admiralty charts and in literature (Jones and Davies 2005).  
179 Semidiurnal signal dominates in the area and the M2 amplitude increases from 0.4 m south of Islay  
180 to 1.1 m in the Tiree Passage. The effects of both long-term seasonal signal and short-term variability  
181 in meteorological forcing are reproduced well by the model. These are well represented in modelled  
182 sea-water Salinity and Temperature fields. These results are presented in Appendix 1.



## 183 2.2 Particle tracking model

184 The particle tracking model was implemented in Java. For these simulations, we used two discrete  
185 periods of the hydrodynamic output: June and October 2011. Wind roses for these periods, based on  
186 a site near the NE corner of subregion 5 in Figure 1, are shown in Figure 2. Wind forcing differed  
187 between the two periods, though both are fairly typical of the study region. June winds are  
188 approximately equally distributed between southerly and north-westerly, while the October winds  
189 are stronger and more predominantly south-westerly. By using two distinct periods of wind forcing,  
190 we hoped to identify patterns that may apply more generally. Wind direction introduces a correlated  
191 dispersal direction in the particle tracking results, which is dealt with in Section 2.5.

192 The region has several areas of very strong tidal flow (up to  $5\text{ms}^{-1}$ ). An hourly update can produce  
193 long range jumps in these areas, producing highly unrealistic tracks. Therefore, a much shorter time  
194 interval ( $\Delta t = 0.005$  hours) was used, linearly interpolating velocities between hourly FVCOM output  
195 values. The distance travelled due to current in one time step is  $\Delta r_{current} = \Delta t \times v$ , where  $v$  is the  
196 current velocity at the location of the larva (the velocity in the closest depth layer and element  
197 centroid; a weighted average of nearest neighbours produced no marked behavioural change).

198 Additional movement due to diffusion was incorporated as  $\Delta r_{diffusion} \sim U(-1, 1) \times \sqrt{6D_h\Delta t}$ , with  
199  $D_h=0.1$  and  $U(-1,1)$  a uniformly distributed random number between -1 and 1. In reality this quantity  
200 varies over space, but difficulties in estimation mean that we use a fixed value  
201 (in line with recent studies such as Amundrud and Murray 2009 and Stucchi et al. 2010).  $r$  and  $v$  are  
202 vector quantities (i.e.  $r=(x,y)$  and  $v=(dx/dt,dy/dt)$ ). The total distance travelled in one timestep was  
203  $\Delta r = \Delta r_{current} + \Delta r_{diffusion}$ . At each timestep, the rule  $r_{t+1} = r_t + \Delta r$  was used to update each  
204 larva's location.

205 To describe connectivity of different parts of the coastline, we considered particle tracks that  
206 connected points on the coastline. The mesh nodes which lie on land boundaries (including islands)  
207 were listed. Working from the start of the full boundary list, nodes were added to a list of viable

208 habitat locations if they did not lie within 1km of a node that was already on the list (giving an even  
209 spread of sites, independent of mesh geometry), leaving 940 “habitat sites”. Particles were released  
210 from the nearest element centroid to each habitat site, and settlement is deemed to have occurred  
211 once a particle moves within 500m of a given site.

212 Each particle becomes “competent” (able to settle) during the latter half of its lifespan; newly  
213 produced larvae of many species are not able to settle successfully. Barnacles, for example, have 6  
214 nauplius stages before the final cyprid settlement stage.

215 At the end of a model run, the start and end locations and duration in hours of all “successful”  
216 trajectories, and the number of “particle-timesteps” spent in each mesh element were recorded.  
217 Particle start and end locations of all other particles are also recorded, in order to identify the  
218 location of those that did not settle at coastal sites (for the calculation of dispersal distance, and to  
219 identify open boundary areas where particle accumulations occur).

220 A range of pelagic larval durations were considered, encompassing that seen in the most common  
221 pelagic dispersing species (summarised by Burrows et al. 2009, Appendix C). The shortest dispersal  
222 duration considered was 1 day, common to many macroalgae species (e.g. *Fucus serratus* L.,  
223 *Ascophyllum nodosum* L.), and the longest 28 days, the approximate duration observed in many  
224 barnacles (e.g. *Semibalanus balanoides* L. (28 days), *Chthamalus montagui* L. (21 days)) and  
225 periwinkles (*Littorina littorea* L. (28 days)).

226 Two types of larvae were considered: (i) particles that remain in the surface layer; and (ii) particles  
227 which alter their depth based on the flooding or ebbing of the tide. The former type could represent  
228 intertidal barnacle nauplii, or sea lice (*Lepeophtheirus salmonis* L.), which tend to be found high in  
229 the water column (Murray and Gillibrand 2006, Tapia et al. 2010). For the latter type, increasing  
230 surface elevation at a particle’s location (element) was taken to indicate local flooding of the tide, in  
231 which case the particle moves to the surface layer. Decreasing surface elevation indicates local

232 ebbing of the tide, and the particle moves into the lowest depth layer. This represents selective tidal  
233 stream transport as observed in later stage larvae of some crustacea (Criales et al. 2011), mussels  
234 (Knights et al. 2006) and plaice (summarised by Fox et al. 2006). This behaviour potentially allows  
235 access to inshore areas that would otherwise be difficult to reach (Sandifer 1975, Knights et al. 2006,  
236 Fox et al. 2006). For each run, 20 particles were released from each habitat site. For larval durations  
237 other than 28 days, particles were split in to cohorts departing on different days spread throughout  
238 the month, to avoid wind patterns early in the month dominating the results.

### 239 **2.3 Coastal metrics**

240 Burrows et al. (2010) used two metrics which aim to quantify the potential connectivity of coastal  
241 sites: “wave fetch” and “openness”. Wave fetch is a sum of straight line distances over open water  
242 measured from a given site, and thus a proxy for the potential distance over which waves can travel  
243 to the site. For each of 16 equal sized angular segments, the nearest other point of coastline within  
244 that segment is identified, up to a maximum of 200km. The maximum possible wave fetch is thus  
245 3200km. Openness is the area of connected sea within a certain radius of a chosen site (here, we use  
246 a slightly different definition and measure the sum of areas of all elements with a mesh centroid  
247 lying closer than the defined radius, here 20km; units  $\text{km}^2$ ). Openness and fetch are generally found  
248 to be strongly correlated, though fetch tends to vary more at small spatial scales. The amount of  
249 open water in the vicinity of a site might be expected to dilute concentrations of released larvae.

250 We also defined a measure of local coastal complexity: “coast length”. This is the length of coastline  
251 within a certain radius (20km) of a target site (units km). In general, measurement of coast length is  
252 defined according to a particular length scale, and here the defined hydrodynamic model mesh is  
253 convenient: the length of closed boundary element edges for elements lying less than 20km away is  
254 summed. This represents the extent of habitat local to each site.

255 Certain strongly tidal areas experience high volumes of water transport which is not adequately  
256 reflected by wave fetch or openness. Given the additional information provided by hydrodynamic

257 simulations, we here consider the average water surface speed (units  $\text{ms}^{-1}$ ). This is the average of all  
258 current velocities in the top layer of the hydrodynamic model and within a certain radius, weighted  
259 by the element areas in which they occur.

260 Viewed through the lens of these metrics, the landscape changes dramatically. This is illustrated by  
261 Figure 3 which plots the relative values of each metric on the coastal habitat sites. The metrics are  
262 plotted against one another in Appendix 2 (Figure A3). Fetch and openness are strongly correlated,  
263 which reduces the effectiveness of regression models. Due to its slightly poorer performance, and  
264 the clear implication of openness in terms of our hypotheses (the dilution effect), fetch will be  
265 dropped in later analyses.

## 266 **2.4 Regression analysis**

267 To assess the impact of coastal topography on dispersal distance, linear models with and without  
268 interaction terms were fitted to the Euclidean distance between each trajectory's start and end  
269 point, using each of the three variables identified in Section 2.3.

270 The coastal site metrics were used in models to predict (i) the number of successful dispersers ("out-  
271 count") and (ii) the number of settlers ("in-count") at each site. In using counts rather than a  
272 mortality-adjusted density, we assume that larval mortality is in proportion with larval duration. We  
273 considered applying a constant rate of mortality over the entire larval duration, and computing the  
274 expected density of successful dispersers/settlers to/from each site (that is, longer dispersers have a  
275 lower probability of success than short dispersers of the same species), but this means that long  
276 larval durations have orders of magnitude difference in probability of successful dispersal. Using  
277 counts directly means that fitted regression parameters are of comparable order for different larval  
278 durations.

279 The number of successful dispersers from each site is essentially a proportion of the maximum  
280 possible, and is bounded by zero and 20. Thus, a GLM using Binomial error structure is implemented

281 to fit these data. The number of arrivals at each site is a count, bounded below at zero; a GLM with  
282 Poisson error structure is fitted here. Models with and without interactions between the explanatory  
283 variables were considered.

284 500 bootstrap samples of the 940 habitat sites were made, and parameters/fit statistics recorded for  
285 each sample to estimate the probability distributions of the fit of the models given different possible  
286 configurations of sites. Boxplots of these distributions are presented throughout Section 3.

## 287 **2.5 Spatial autocorrelations**

288 Early tests indicated that prevailing South-Westerly/Easterly winds induced spatial correlation in  
289 dispersal patterns (Figure 4), with a general northward flow of particles observed. Settlement is  
290 biased towards sites at the north end of the region. In the study region, location correlates with the  
291 environmental variables, and so geographic subsets of the region were considered. Three  
292 longitudinal three and latitudinal divisions (equal) were imposed, and individual regressions to out-  
293 and in-counts were performed for each sub-region cell. Only regions containing sufficiently many  
294 habitat points, with a broad range of coastal properties, are included in the analysis. We thus  
295 excluded the bottom row and left column of the geographic subsets (cells 1, 2, 3, 4 and 7; see Figure  
296 1 and Figure 4). For fits to the entire domain, spatial plots of residuals and semivariograms were also  
297 used to check for trends.

## 298 **3 RESULTS**

299 In all fitted models, the high correlation between wave fetch and openness was found to reduce the  
300 predictive power of either. Fetch generally explained a somewhat lower proportion of deviance, and  
301 was found to have a high Variance Inflation Factor. It is thus removed for the analyses considered in  
302 this section (following the recommendation of Zuur et al., 2009). Only minor differences were seen  
303 between the fits for June 2011 and the fits to October 2011 model output (see figures and

304 explanations in Appendix 2), and so for simplicity all results presented in this section relate to model  
305 output for June 2011.

306 At short larval durations, simple additive models generally offer good fits to distance travelled,  
307 number of successful departures or arrivals, with interaction terms explaining only a small part of  
308 the variation. At long larval durations, interaction terms become increasingly important; a  
309 consequence of the interaction between the coastline and heterogeneous wind forcing.

### 310 **3.1 Dispersal distance**

311 Using an additive linear model excluding interaction between explanatory variables, it is found that  
312 dispersal has a significant relationship with site openness (positive, Figure 5a) and average  
313 neighbourhood current speed (positive: Figure 5c, and see also Appendix 2.1). Velocity explains the  
314 largest portion of variance, followed by openness. For longer larval durations (>4 days), dispersal  
315 distance was also significantly negatively correlated with coast length.

316 The same patterns hold across all larval durations. In order of importance, high velocity, high  
317 openness and low coast length (especially in combination) provide suitable conditions for longer  
318 dispersal distances. For example, with 8 day dispersal, the median distance from high velocity sites  
319 was 30km, three times that of the lowest velocity sites. High openness sites produced at most a  
320 twofold increase in median dispersal distance, while the effect of coast length is not clear from  
321 figures (see Figure 5).

322 Simple additive models explained up to 47% of the variance ( $R^2$ ), while models including all possible  
323 interaction terms explained slightly more of the variance (up to 56%). The  $R^2$  of the model including  
324 the additive terms and a two-way interaction between velocity and coast length (negative response)  
325 was at worst 2% lower than the model containing all possible (up to 3-way) interactions (see  
326 Appendix 2, Figure 4).

## 327 3.2 Site fluxes in simulations without vertical behaviour

### 328 3.2.1 Proportion of successful dispersal events (“out-count”)

329 Outgoing dispersal success is fitted best for short to moderate duration dispersal (2-4 days, max  
330 deviance explained by an additive model c48%). This reflects the fact that after a lengthy period in  
331 the water column, the location of larvae becomes relatively uncorrelated with their natal site, being  
332 more influenced by wind and tide driven current patterns encountered along the way. Furthermore,  
333 at the longest larval durations, a high proportion of the dispersing particles are successful. This  
334 reduces the predictive power of additive models and produces a more complicated array of  
335 interaction terms, which have increasing importance as larval duration increases.

336 In the additive model, significant relationships are found between the number of successful  
337 dispersers from a site and all variables, the most important being openness (negative relationship,  
338 Figure 6e). The relationship with coast length is positive (Figure 6f), and with velocity negative,  
339 except for the longest larval duration (Figure 6g). Median dispersal success is generally high (for  
340 example, 8 day dispersal the median proportion finding settlement sites is around 0.8), and major  
341 deviations from this are only seen for high openness sites (median success as low as 20% for the  
342 highest openness sites at 8 days – not shown). This supports the hypothesis that larvae from open  
343 and exposed sites are more likely to be “lost at sea”. The positive relationship with coast length  
344 aligns with the hypothesis that increased availability of downstream habitat should increase the  
345 probability of successful dispersal.

346 The relative importance of the terms may be measured and easily visualised by considering the  
347 proportional loss of deviance explained by the model when each of the terms is dropped (“drop1”  
348 function in R; Chambers & Hastie 1992). Openness arises as the most influential term, particularly at  
349 short larval duration (Figure 6 b,c,d). As larval duration increases, so does the relative importance of  
350 coast length and velocity (though openness remains the most important). Dilution of particles at  
351 open sites appears to dominate the patterns.

352 Considering fits within the cells 5, 6, 8, and 9 identified in Figure 1, a slightly more nuanced picture  
353 emerges (results not shown). Openness remains dominant, but for particles with very long larval  
354 durations, has a positive effect on dispersal in cell 5 (the only region for which substantial  
355 “downwind” habitat exists in the model domain). The effect of coast length on outgoing success  
356 remains positive, unless the coastline “faces” the prevailing wind (cell 5). Velocity has a negative  
357 effect on out-count at short larval durations but becomes increasingly positive for “upwind” areas at  
358 longer larval durations, until a positive relationship dominates (matching the full region result).  
359 These are all important reasons why simple metrics have limited predictive power in relation to  
360 exact dispersal patterns.

361 In general, interaction models for out-count contain many highly non-significant terms (even in the  
362 geographical cell fits), and while the proportion of deviance explained by the model improves, the  
363 greatest improvement is 6% of the total deviance (over 19% by the additive model for 28 day  
364 dispersal; see Appendix 2, Figure 5).

### 365 **3.2.2 Cumulative arrival of settling larvae (“In-count”)**

366 There were notable outliers in the number of particles arriving at the habitat sites. In particular,  
367 these occurred at the north of the model, where the islands of Coll and Tiree meet the open  
368 boundaries. Particles cannot leave the model domain, and when reaching close proximity to a  
369 boundary generally become constrained by the model boundary. If the model domain were larger,  
370 such particles would move further north, outside of the current domain. Other large accumulations  
371 of larval particles are noted at the northern end of the western open boundary, below the southern  
372 tip of Tiree. These patterns of accumulation and movement are due to the large quantity of coastal  
373 habitat in the Firth of Lorn region, and the dominant flow patterns, which the model appears to  
374 represent well. However, such points are discounted as outliers in the following analysis (sites with  
375 in-counts greater than  $\mu+3\sigma$ ).



376 The overall ability of the metrics to explain in-count at coastal sites is somewhat lower (c10%  
377 deviance explained: see Figure 7a and Appendix 2, Figure A6), but relationships are generally  
378 significant. Interactions again have high importance for longer larval durations reflecting the  
379 increasing importance of wind forcing and overall current patterns as larvae spend longer in the  
380 water column. However, up to 8 day dispersal, the additive model of coast length and velocity  
381 explains around 75% of the deviance explained by the full 3-way interaction model (see Appendix 2,  
382 Figure A6), and these are certainly the most important terms in the additive model at shorter larval  
383 durations (Figure 7 b,c,d). At longer durations, openness becomes the most important term and has  
384 a positive impact on the number of arrivals, primarily in interaction with low velocity (Appendix 2,  
385 Figure A6). Velocity and coast length have impacts of similar magnitude on the number of arrivals  
386 (not shown). Up to twice as many particles arrive at the lowest velocity sites compared with the  
387 highest (medians for 4 day dispersal 17 versus 7). For 2 day dispersal, the median number of arrivals  
388 for the longest coast length sites is 15, and for the lowest, 3. These are extreme cases, but are  
389 indicative of the general patterns observed.

390 Fits to sites within the geographic cells show similar patterns. However, response to openness is  
391 always positive in some cells (5, 9). It becomes positive in 8 at long durations, too, but never in 6 (the  
392 cell contains many SW facing narrow sea lochs, which perhaps explains a tendency for settlement to  
393 occur in low openness regions). Response to coast length is always negative, except at very short  
394 and long larval durations in cell 9. Response to velocity remains negative in all cells except 6. This  
395 gives useful support to the generality of the results.

396 Spatial plots of model residuals indicated no clear trend on the scale of the domain. By virtue of their  
397 location within the domain, certain areas receive larger numbers of arriving larvae than is predicted  
398 by the model (particularly the Corryvreckan area and the north end of the Sound of Mull; Appendix  
399 2, Figure A12). Semivariograms (indicating average variation in residuals over all possible spatial  
400 separations) indicated that variation at small scales (less than 15-20km) is generally smaller than

401 that at larger scales, further supporting the idea that recruitment is enhanced in proximity to  
402 particular features of the domain (Appendix 2, Figure A13).

### 403 **3.3 Site fluxes with vertical migration: surface on flood tide, bed on ebb**

#### 404 **3.3.1 General implications**

405 Current speed (and often direction) varies over the water column, with the fastest currents generally  
406 occurring close to the surface. These currents are also those most closely related to wind direction.  
407 Both factors mean that vertical migration behaviour alters larval dispersal patterns. In model  
408 simulations, particles that migrate to surface waters on the flood tide and the sea bed on the ebb  
409 tide were found to generally travel shorter distances than (but experience similar success in reaching  
410 suitable settlement habitat sites to) those that inhabit only surface waters (Figure 8). At  
411 intermediate durations (8 day dispersal), more vertically migrating particles settle successfully under  
412 June 2011 wind forcing. Vertical migration of this type also results in more particles being retained  
413 close to the shore (Appendix 2, Figure A7), but not the same “estuary homing” behaviour seen by  
414 Fox et al. (2009). There did not appear to be dramatic differences in the influence of the different  
415 coastal variables on dispersal success, but some finer details are outlined below.

#### 416 **3.3.2 Dispersal success**

417 Including vertical migration behaviour gives very similar relationships to the case where particles  
418 inhabit the surface layer only. Velocity becomes more important (and overall the model performs  
419 better) at long larval durations, than in the surface only model (see Appendix 2, Figure A8).

#### 420 **3.3.3 Number of arriving larvae**

421 The number of arrivals of vertically migrating particles is affected much more by openness at short  
422 larval duration than in the surface only case. Otherwise, patterns of importance are similar, though  
423 velocity is never quite as important as in the surface only case (see Appendix 2, Figure A9).

### 424 3.4 Comparison with locally observed taxa

425 How do our model results compare with the distributions of locally observed organisms? In making  
426 any comparisons, it only makes sense to compare the abundance of species that disperse pelagically,  
427 and tend to be limited by recruitment, as opposed to processes operating on the adult stage of the  
428 life cycle, such as food availability.

429 Figure 9a shows the abundance (measured on the SACFOR scale; Joint Nature Conservation  
430 Committee 2013, data from Burrows et al., 2009) of adult individuals of a barnacle with a 21-day  
431 pelagic dispersal phase, *Chthamalus montagui* L.. Patterns in abundance of adult barnacles  
432 correspond well with those in abundance of model particles settling on the coastline (Figure 9b,c)  
433 West of Jura, close to the Corryvreckan, and at the northern end of the sound of Mull are higher  
434 density regions both in the model and in reality. On Islay, low density regions are also seen on the  
435 northwest coast and higher densities in the south-western embayment in both the model and  
436 observed abundance. A similar distinction can be made between sites in the main body of Loch  
437 Linnhe (the main inlet; relatively high densities) and its subsidiary lochs (low densities), in both the  
438 observed abundances of *Chthamalus* and modelled arrivals with 16 day larval duration. Rank  
439 correlation tests between observed abundances of *Chthamalus* and average model arrival rates  
440 within a 10km radius of a survey site were strongly significant (Kruskal test, p-value 0.02).

441 Patterns of abundance of the dominant barnacle in the region *Semibalanus balanoides* L. (28 day  
442 dispersal) were not easily comparable with model output, since observed densities fell into the  
443 “abundant” category ( $1-3\text{cm}^{-2}$ ) at the vast majority of sites, though the only site where it was absent  
444 was coincident with one of the lowest arrival areas in the model (not shown).

## 445 4 DISCUSSION AND IMPLICATIONS

### 446 4.1 Discussion

447 Particle-tracking models are now an established method of understanding hydrodynamic  
448 connectivity, which have been used in many different scenarios with both physical and biological  
449 applications. However, this is the first study that has sought to relate predicted connectivity of  
450 coastal populations to derived descriptive measures of coastline geography, such as wave fetch and  
451 openness (Burrows et al. 2008, 2010). Our goal was to understand whether such metrics might be  
452 used effectively as a surrogate for the larval dispersal predictions of a hydrodynamic particle-  
453 tracking model. While it is clear that these metrics explain up to around 50% of the variation in  
454 connectedness among coastline cells in our model (depending the on metric of interest), much of  
455 the pattern of connections is not predicted by our coastline metrics. In particular, the success of  
456 dispersing particles is much better predicted than the number of arriving particles.

457 Three quantities that summarise the dispersal potential of coastal sites were considered: distance  
458 dispersed, number of successful departing dispersers, and number of arriving particles. As expected,  
459 distance travelled was most closely related to local current velocity (positively). The fitted signs of  
460 the other terms (openness, positive; coast length, negative) were also in agreement with our initial  
461 hypothesis. The success of dispersing particles was most closely related to openness of the source  
462 site – particles from more open areas experiencing reduced success in reaching settlement sites.  
463 Coast length had a positive impact on success, velocity a negative impact. Both distance dispersed  
464 and success were well explained by simple additive models of openness, coast length and velocity,  
465 which made the results easy to interpret. The best-fitting models were in agreement with our initial  
466 hypotheses.

467 Influx at a given site was poorly predicted by our indices of coastal geography. After removing  
468 outliers, models (up to three-way interaction) never explained more than 11% of the deviance. Coast  
469 length and velocity were the most important terms in additive models, but at longer larval durations

470 the interactions between terms dominated the patterns. For these particles, the manner in which  
471 current systems and variable meteorological conditions interact with coastline topography may  
472 ultimately have the strongest influence on settlement density, as represented by particle influx.

473 We expected that tidal vertical migration might have increased the success of particles in reaching  
474 suitable coastal habitat. We found this to be the case at only one of the tested larval durations (8  
475 days). A study by Fox et al. (2006) found that tidal vertical migration helped fish larvae to accumulate  
476 in bays and estuaries that would have been otherwise much less accessible, but there are some  
477 notable differences between Fox's model and this study. In our model the changing tide direction  
478 (flood/ebb) simply caused a switch in vertical position (ignoring actual migration speed and timing),  
479 while Fox's study implements vertical movement of particles. The latter is undoubtedly more  
480 realistic, though our configuration was intended to provide simplified limiting case; that we do not  
481 see a similarly strong effect of vertical migration is slightly surprising. The difference between the  
482 two geographical areas may play a role in the differences. The northern Irish Sea has extensive  
483 shallow areas on the eastern (Lancashire) and southern margin (North Wales) where selectively  
484 tidally migrating larvae may accumulate, while the Firth of Lorn lack marginal shallows, being deeply  
485 divided by glacial cut tidal channels with strong flow, so vertical movement may have little influence  
486 on ultimate locations.

487 The model's reflecting boundaries, and the persistent southerly and south-westerly winds  
488 experienced by this region (of which the study periods are fairly typical) are likely to ensure that  
489 many of the longer-lived particles produced in the model domain accumulate in regions to the north  
490 around Coll and Tiree. This may help to explain the frequent presence of large filter feeders such as  
491 Basking sharks (*Cetorhinus maximus L.*) in these areas (Witt et al. 2012). To determine whether these  
492 really are likely to be accumulation zones or are simply an artefact of the model domain would  
493 require a larger scale model in which particles do not attempt to exit the domain.

494 In order to improve the credibility of our results, we carried out identical analyses for two distinct  
495 modelled periods of time. Meteorological forcing and consequently hydrodynamic currents  
496 (particularly at the surface) differed between the two periods. This led to slight differences in the  
497 importance of the three coastal variables included in the analysis. However, no fundamental  
498 changes were observed. Changes in larval duration had a greater impact on the importance of  
499 coastal features than did changes in the wind forcing. While certain areas do lend themselves to  
500 efficient spread or accumulation of particles, meteorology can always be expected to play a central  
501 role in the success or failure of recruitment over a particular period, at a particular site. A single  
502 extreme weather event may lead to dramatic deviations from usual levels of larval abundance,  
503 though this of course depends on the duration of the “pulse” over which larvae are released.  
504 Prediction of variation in larval abundance in all but the simplest systems will thus continue to  
505 require a detailed understanding of meteorology and local hydrodynamics over the period of  
506 interest.

507 Given the many processes involved in marine organisms’ life cycles, and the imperfect  
508 representation of natal habitat (inhomogeneous in reality) it would perhaps be unreasonable to  
509 expect modelled larval supply values to align perfectly with abundances observed in the field.  
510 Nevertheless, the visual comparison possible using Figure 9 seems to suggest that dispersal patterns  
511 in the model are similar to those that might occur in reality. Differences in abundance observed both  
512 in general areas of the model domain and in specific features (embayments and subsidiary lochs, for  
513 example) are represented well in many cases, lending further support to our findings.

## 514 **4.2 Implications**

515 For short to medium duration larval durations, openness has a negative effect on dispersal success,  
516 exacerbated by rapid velocities, another negative effect. The amount of ‘target’ habitat positively  
517 influences success. This means that the larvae of species living on headlands and islands are less  
518 likely to reach other coastlines than those living along sheltered and enclosed coasts. On the other

519 hand, dispersal distance was up to twice as far from open sites, increasing the spatial scale of  
520 connectedness for species on the open coast. Dispersal distance defines the minimum spatial scale  
521 at which populations can be considered as 'closed' (as in Roughgarden's model). This study makes it  
522 clear that this concept can only reasonably be applied to the particular situation where adults living  
523 in sheltered locations produce larvae with short dispersal duration; otherwise, external sources of  
524 larvae must be invoked.

525 That the influx of settling particles (in-count) was poorly predicted by simple measures of coastline  
526 geography, and more likely to be driven by local meteorological forcing interacting with coastal  
527 configurations is well in line with other observations around the world  
528 (Bertness et al. 1996; Hawkins and Hartnoll 1982; Perry et al. 1995), that emphasise stochastic or  
529 temporal variation in larval supply (Pineda et al. 2006). Underwood and Fairweather (1989) point  
530 out the practical implications of this: wide variation in population structure occurring under similar  
531 conditions – it is simply a case of who arrives first. Looking at our results for the entire coastline in  
532 the region, the modal success of dispersing larvae from all sites was 100%. However, in all but the 1  
533 day dispersal case, the modal number of arrivals per site was zero. Our model therefore suggests  
534 that relatively low settlement is likely to be ubiquitous, with localised "hotspots". This contrasts  
535 with the situation for dispersal success, which is reasonably even throughout the study region.  
536 Sources to the broader larval pool are common, but sinks are much rarer. In reality, larvae may  
537 reject empty sites, settling in response to the detection of pheromones (so called "gregarious  
538 settlement"; Burke 1986), or be unable to settle at full sites (Todd et al. 2006), increasing the spatial  
539 spread of larvae and mitigating this "hotspot" effect.

540 The relationship between openness and settlement is an interesting one. At a broad scale, our  
541 models predicted a positive relationship. However, within smaller geographic sub-regions (reducing  
542 the impact of wind induced spatial correlations) a negative relationship was generally observed.  
543 Thus, for open coastal species, settlement density and recruitment to adult populations is likely to

544 be less, reducing the impact of intra-specific competition and other negative density dependent  
545 effects, such as prey-switching predators (Menge and Sutherland 1987). In contrast, species living at  
546 less open sites are more likely to be successful in their reproductive output, with larvae much more  
547 likely to reach suitable habitat at a shorter distance away. Settlement densities are likely to be high,  
548 and competition for space may be a more important driving factor. Connell's populations of  
549 *Semibalanus balanoides* in the Firth of Clyde (Connell 1961) are a good example of populations in a  
550 low openness region, and his very high settlement densities (c.80 larvae cm<sup>-2</sup>) must have been  
551 caused by the restricted dispersal evident in part of our model domain. High settlement densities  
552 causes unstable "hummocks" of crowded barnacles that are often sloughed from the rock surface in  
553 the first year of life (Barnes and Powell 1950; Bertness et al. 1998), increasing mortality rates and  
554 producing more space available for settlement in the following year (Jenkins et al. 2008).

555 With respect to the relationship between larval duration and habitat "preference", our model seems  
556 to suggest that longer duration larvae are more likely to settle in open areas, and those with low  
557 coast length (habitat availability) than are short duration larvae. This lends further credence to the  
558 ideas of (Crisp et al. 1982). However, it would seem that high openness always has a negative effect  
559 on the success of dispersing larvae, while coast length always has a positive effect.

560 The characteristics that allow species to reach and colonize novel habitats are not entirely clear. Our  
561 results clearly show that species with longer larval durations are likely to have greater mean  
562 dispersal range, as are those that inhabit open and exposed areas of shoreline. However, ability to  
563 disperse does not imply ability to colonise. Without greatly increased levels of larval production, long  
564 distance dispersers become more diffuse, and are thus likely to find themselves at much lower  
565 settlement densities than short dispersers. This increases their susceptibility to Allee effects  
566 (Gascoigne and Lipcius 2004), since finding mates and thereby reproduction is more difficult at low  
567 population densities, particularly when colonising new areas. Understanding these effects may be



568 possible using dynamic models that encompass organisms' entire lifecycles, but empirical  
569 observations made as conditions change are certain to reveal some surprises.

## 570 **5 ACKNOWLEDGEMENTS**

571 This work was carried out as part of the Marine Renewable Energy and the Environment (MaREE)  
572 project which is supported by funding from Highlands and Island Enterprise, the Scottish Funding  
573 Council and the European Regional Development Fund. Hydrophysical model development was  
574 supported by EU FP7 projects ASIMUTH (Grant No 261860) and HYPOX (Grant No 226213). We are  
575 grateful for the comments of two anonymous referees which helped substantially improve the  
576 manuscript.

## 577 6 REFERENCES

- 578 Adams, T. P. et al. 2012. Connectivity modelling and network analysis of sea lice infection in Loch  
579 Fyne, west coast of Scotland. - *Aquaculture Environment Interactions* 3: 51–63.
- 580 Aiken, C. M. et al. 2007. Along-shore larval dispersal kernels in a numerical ocean model of the  
581 central Chilean coast. - *Marine Ecology Progress Series* 339: 13–24.
- 582 Amundrud, T. L. and Murray, A. G. 2009. Modelling sea lice dispersion under varying environmental  
583 forcing in a Scottish sea loch. - *Journal of Fish Diseases* 32: 27–44.
- 584 Ayata, S. et al. 2010. How does the connectivity between populations mediate range limits of marine  
585 invertebrates? A case study of larval dispersal between the Bay of Biscay and the English  
586 Channel (North-East Atlantic). - *Progress in Oceanography* 87: 18–36.
- 587 Barnes, H. and Powell, H. T. 1950. The Development, General Morphology and Subsequent  
588 Elimination of Barnacle Populations, *Balanus crenatus* and *B. Balanoides*, After a Heavy  
589 Initial Settlement. - *Journal of Animal Ecology* 19: 175–179.
- 590 Bertness, M. et al. 1996. Wind driven settlement patterns in the acorn barnacle *Semibalanus*  
591 *balanoides*. - *Marine Ecology Progress Series* 137: 103–110.
- 592 Bertness, M. D. et al. 1998. Making mountains out of barnacles: the dynamics of acorn barnacle  
593 hummocking. - *Ecology* 79: 1382–1394.
- 594 Blumberg, A. F. and Mellor, G. L. 1987. A description of a three-dimensional coastal ocean circulation  
595 model. - *Coastal and estuarine sciences* 4: 1–16.
- 596 Brown, J. H. 1984. On the Relationship between Abundance and Distribution of Species. - *The*  
597 *American Naturalist* 124: 255–279.

- 598 Burke, R. D. 1986. Pheromones and the gregarious settlement of marine invertebrate larvae. -  
599 Bulletin of Marine Science 39: 323–331.
- 600 Burrows, M. T. et al. 2008. Wave exposure indices from digital coastlines and the prediction of rocky  
601 shore community structure. - Marine Ecology Progress Series 353: 1–12.
- 602 Burrows, M. T. et al. 2009. Spatial scales of variance in abundance of intertidal species: effects of  
603 region, dispersal mode, and trophic level. - Ecology 90: 1242–1254.
- 604 Burrows, M. T. et al. 2010. Spatial variation in size and density of adult and post-settlement  
605 *Semibalanus balanoides*: effects of oceanographic and local conditions. - Marine Ecology  
606 Progress Series 306: 207–219.
- 607 Chambers, J. M. and Hastie, T. J. 1992. Linear models. Chapter 4 of Statistical Models in S. -  
608 Wadsworth and Brooks/Cole.
- 609 Chen, C. et al. 2003. An Unstructured Grid, Finite-Volume, Three-Dimensional, Primitive Equations  
610 Ocean Model: Application to Coastal Ocean and Estuaries. - Journal of Atmospheric and  
611 Oceanic Technology 20: 159–186.
- 612 Connell, J. H. 1961. Effects of Competition, Predation by *Thais lapillus*, and Other Factors on Natural  
613 Populations of the Barnacle *Balanus balanoides*. - Ecological Monographs 31: 61–104.
- 614 Costello, M. 2009. How sea lice from salmon farms may cause wild salmonid declines in Europe and  
615 North America and be a threat to fishes elsewhere. – Proceedings of The Royal Society B  
616 276: 3385–3394.
- 617 Criales, M. M. et al. 2011. Field Observations on Selective Tidal-Stream Transport for Postlarval and  
618 Juvenile Pink Shrimp in Florida Bay. - Journal of Crustacean Biology 31: 26–33.

- 619 Crisp, D. J. et al. 1982. On the distribution of the intertidal barnacles *Chthamalus stellatus*,  
620 *Chthamalus montagui* and *Euraphia depressa*. - *Journal of the Marine Biological Association*  
621 *of the United Kingdom* 61: 359–380.
- 622 Dobretsov, S. V. and Miron, G. 2001. Larval and post-larval vertical distribution of the mussel *Mytilus*  
623 *edulis* in the White Sea. - *Marine Ecology Progress Series* 218: 179–187.
- 624 Edwards, A. and Sharples, F. 1986. *Scottish Sea Lochs: A Catalogue*. - *Scottish Marine Biological*  
625 *Association*.
- 626 Egbert, G. D. et al. 2010. Assimilation of altimetry data for nonlinear shallow-water tides: Quarter-  
627 diurnal tides of the Northwest European Shelf. - *Continental Shelf Research* 30: 668–679.
- 628 Fox, C. J. et al. 2006. The importance of individual behaviour for successful settlement of juvenile  
629 plaice (*Pleuronectes platessa* L.): a modelling and field study in the eastern Irish Sea. -  
630 *Fisheries Oceanography* 15: 301–313.
- 631 Fox, C. J. et al. 2009. Potential transport of plaice eggs and larvae between two apparently self-  
632 contained populations in the Irish Sea. - *Estuarine, Coastal and Shelf Science* 81: 381–389.
- 633 Gaines, S. D. et al. 2003. Avoiding current oversights in marine reserve design. - *Ecological*  
634 *Applications* 13: 32–46.
- 635 Gaines, S. D. et al. 2007. Connecting places: The ecological consequences of dispersal in the sea. -  
636 *Oceanography* 20: 90–99.
- 637 Gascoigne, J. and Lipcius, R. N. 2004. Allee effects in marine systems. - *Mar Ecol Prog Ser* 269: 49–59.
- 638 Gillibrand, P. and Willis, K. 2007. Dispersal of sea louse larvae from salmon farms: modelling the  
639 influence of environmental conditions and larval behaviour. - *Aquatic Biology* 1: 63–75.

- 640 Grosberg, R. K. 1982. Intertidal Zonation of Barnacles: The Influence of Planktonic Zonation of Larvae  
641 on Vertical Distribution of Adults. - *Ecology* 63: 894–899.
- 642 Hawkins, S. J. and Hartnoll, R. G. 1982. Settlement patterns of *Semibalanus balanoides* (L.) in the Isle  
643 of Man (1977-1981). - *Journal of Experimental Marine Biology and Ecology* 62: 271–283.
- 644 Huang, H. et al. 2008. FVCOM validation experiments: Comparisons with ROMS for three idealized  
645 barotropic test problems. - *Journal of Geophysical Research: Oceans* 113: n/a–n/a.
- 646 Ivanov, V. et al. 2011. A high-resolution baroclinic model of Loch Linnhe.
- 647 Jenkins, S. R. et al. 2008. Temporal changes in the strength of density-dependent mortality and  
648 growth in intertidal barnacles. - *Journal of Animal Ecology* 77: 573–584.
- 649 Joint Nature Conservation Committee 2013. SACFOR abundance scale used for both littoral and  
650 sublittoral taxa from 1990 onwards.
- 651 Jones, J. and Davies, A. 2005. An intercomparison between finite difference and finite element  
652 (TELEMAC) approaches to modelling west coast of Britain tides. - *Ocean Dynamics* 55: 178–  
653 198.
- 654 Knights, A. M. et al. 2006. Mechanisms of larval transport: vertical distribution of bivalve larvae  
655 varies with tidal conditions. - *Marine Ecology Progress Series* 326: 167–174.
- 656 Kot, M. et al. 1996. Dispersal data and the spread of invading organisms. - *Ecology* 77: 2027–2042.
- 657 Kristoffersen, A. B. et al. Understanding sources of sea lice for salmon farms in Chile. - *Preventive*  
658 *Veterinary Medicine* in press.
- 659 Largier, J. L. 2003. Considerations in estimating larval dispersal distances from oceanographic data. -  
660 *Ecological Applications* 13: 71–89.

- 661 Mellor, G. and Yamada, T. 1982. Development of a turbulence closure model for geophysical fluid  
662 problems. - *Reviews of Geophysics and Space Physics* 20: 851–875.
- 663 Menge, B. A. and Sutherland, J. P. 1987. Community Regulation: Variation in Disturbance,  
664 Competition, and Predation in Relation to Environmental Stress and Recruitment. - *The*  
665 *American Naturalist* 130: 730–757.
- 666 Mitarai, S. et al. 2009. Quantifying connectivity in the coastal ocean with application to the Southern  
667 California Bight. - *Journal of Geophysical Research* 114: C10026.
- 668 Muko, S. and Iwasa, Y. 2000. Species Coexistence by Permanent Spatial Heterogeneity in a Lottery  
669 Model. - *Theoretical Population Biology* 57: 273–284.
- 670 Murray, A. G. and Gillibrand, P. A. 2006. Modelling salmon lice dispersal in Loch Torridon, Scotland. -  
671 *Marine pollution bulletin* 53: 128–135.
- 672 North, E. et al. 2008. Vertical swimming behavior influences the dispersal of simulated oyster larvae  
673 in a coupled particle-tracking and hydrodynamic model of Chesapeake Bay. - *Marine Ecology*  
674 *Progress Series* 359: 99–115.
- 675 Perry, H. M. et al. 1995. Settlement Patterns of *Callinectes Sapidus Megalopae* in Mississippi Sound:  
676 1991, 1992. - *Bulletin of Marine Science* 57: 821–833.
- 677 Pineda, J. et al. 2006. Timing of successful settlement: demonstration of a recruitment window in the  
678 barnacle *Semibalanus balanoides*. - *Marine Ecology Progress Series* 320: 233–237.
- 679 Pineda, J. et al. 2007. Larval transport and dispersal in the coastal ocean and consequences for  
680 population connectivity. - *Oceanography* 20: 22–38.
- 681 Possingham, H. P. and Roughgarden, J. 1990. Spatial population dynamics of a marine organism with  
682 a complex life cycle. - *Ecology* 71: 973–985.

683 Radford, C. A. et al. 2011. Juvenile coral reef fish use sound to locate habitats. - *Coral Reefs* 30: 295–  
684 305.

685 Rio Doce, A. P. C. et al. 2008. A finite element method to solve a population dynamics stage-  
686 structured model of intertidal barnacles. - *Ecological Modelling* 214: 26–38.

687 Robins, P. E. et al. 2013. Physical and biological controls on larval dispersal and connectivity in a  
688 highly energetic shelf sea. - *Limnol. Oceanogr* 58: 000–000.

689 Roughgarden, J. et al. 1985. Demographic theory for an open marine population with space-limited  
690 recruitment. - *Ecology* 66: 54–67.

691 Sandifer, P. A. 1975. The role of pelagic larvae in recruitment to populations of adult decapod  
692 crustaceans in the York River estuary and adjacent lower Chesapeake Bay, Virginia. -  
693 *Estuarine and Coastal Marine Science* 3: 269–279.

694 SeaZone 2007. SeaZone Hydrospatial Charted Vector, Digital Survey Bathymetry & Charted Raster  
695 User Guide (Version 1.1e). - EDINA Digimap.

696 Siegel, D. et al. 2003. Lagrangian descriptions of marine larval dispersion. - *Marine Ecology Progress*  
697 *Series* 260: 83–96.

698 Smagorinsky, J. 1963. General circulation experiments with the primitive equations. - *Monthly*  
699 *Weather Review* 91: 99–164.

700 Stucchi, D. J. et al. 2010. Modeling Sea Lice Production and Concentrations in the Broughton  
701 Archipelago, British Columbia. - *Salmon Lice*: 117–150.

702 Sundelöf, A. and Jonsson, P. R. 2011. Larval dispersal and vertical migration behaviour—a simulation  
703 study for short dispersal times. - *Marine Ecology* 33: 1–11.

704 Tapia, F. J. et al. 2010. Vertical distribution of barnacle larvae at a fixed nearshore station in southern  
705 California: Stage-specific and diel patterns. - *Estuarine, Coastal and Shelf Science* 86: 265–  
706 270.

707 Todd, C. D. et al. 2006. Improvements to a passive trap for quantifying barnacle larval supply to  
708 semi-exposed rocky shores. - *Journal of Experimental Marine Biology and Ecology* 332: 135–  
709 150.

710 Treml, E. A. et al. 2008. Modeling population connectivity by ocean currents, a graph-theoretic  
711 approach for marine conservation. - *Landscape Ecology* 23: 19–36.

712 Underwood, A. J. and Fairweather, P. G. 1989. Supply-side ecology and benthic marine assemblages.  
713 - *Trends in Ecology & Evolution* 4: 16–20.

714 Witt, M. J. et al. 2012. Basking sharks in the northeast Atlantic: spatio-temporal trends from  
715 sightings in UK waters. - *Marine Ecology Progress Series* 459: 121–134.

716 Zhao, L. et al. 2006. Tidal flushing and eddy shedding in Mount Hope Bay and Narragansett Bay: An  
717 application of FVCOM. - *Journal of Geophysical Research: Oceans* 111: n/a–n/a.

718 Zuur, A. F. et al. 2009. A protocol for data exploration to avoid common statistical problems. -  
719 *Methods in Ecology and Evolution* 1: 3–14.

720



721 **7 SUPPORTING INFORMATION**

722 Additional Supporting Information may be found in the online version of this article:

723 **Appendix 1** Hydrodynamic model detail.

724 **Appendix 2** Particle tracking results – Supplementary figures.

725

## 726 **8 FIGURE LEGENDS**

727 Figure 1: Finite element mesh of study area. Such a mesh allows spatial variation in model  
728 resolution, essential for accurate and computationally efficient representation of regions with  
729 complex coastlines. The mesh is overlaid with a grid showing the geographic subdivisions discussed  
730 in Section 2.5; a cross in the lower left corner indicates that the cell was excluded from that analysis.  
731 The number of coastal habitat sites (Section 2.2) in each of these is given in the bottom right corner.

732 Figure 2: Wind roses of direction and speed ( $\text{ms}^{-1}$ ) for the two months considered for larval dispersal,  
733 June and October 2011, interpolated from several weather stations to a point in the NE of sub-  
734 region 5.

735 Figure 3: Relative values of the metrics (a) openness, (b) coast length and (c) velocity, plotted at each  
736 habitat site. Black indicates a relatively high value of the metric, white relatively low. The distribution  
737 of values and spatial scale of variation differs between the metrics.

738 Figure 4: Coastal metrics by geographic subdivision: (a) openness, (b) coast length and (c) velocity.  
739 Subregions 5, 6, 8 and 9 have the most desirable combination of ample data points and broad range  
740 of metrics. Boxplots show the median (thick horizontal line), interquartile range (box limits) and 95  
741 percentiles (whiskers).

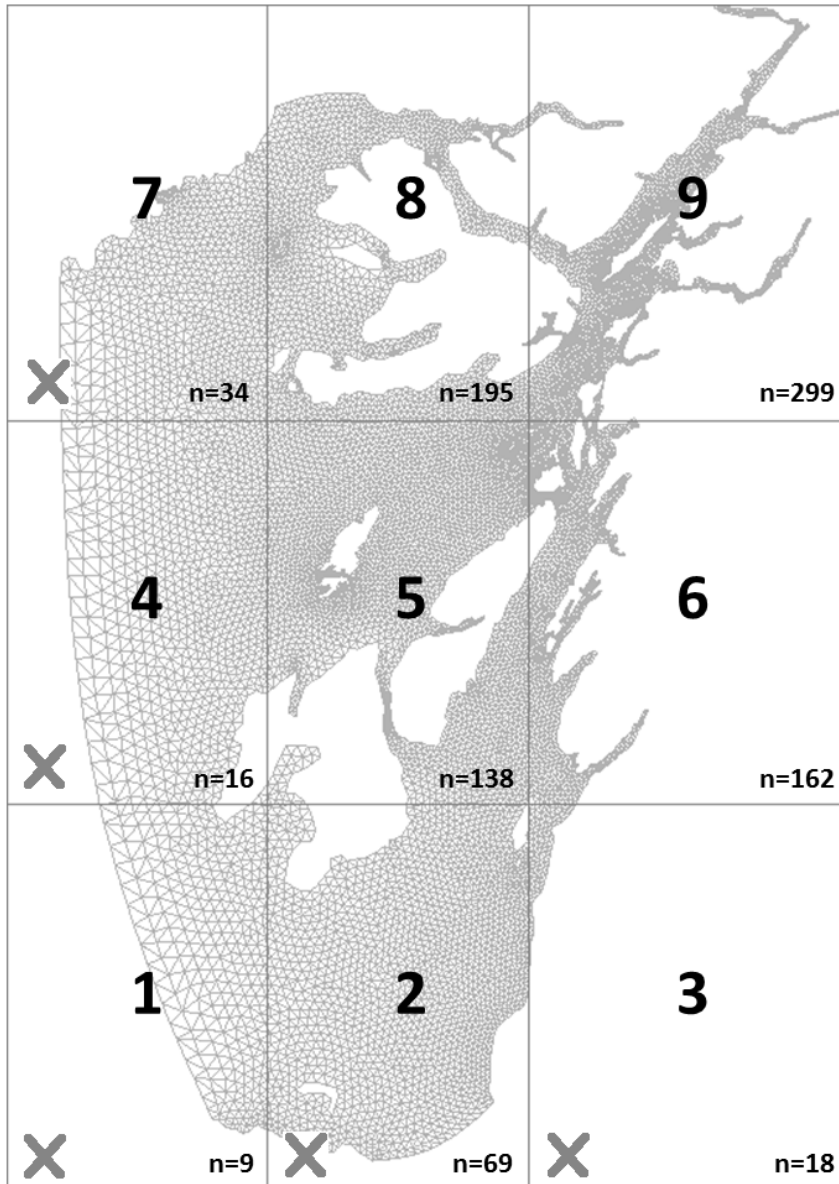
742 Figure 5: Distance travelled (whether settled or not) versus source site metric, for 8 day PLD: (a)  
743 openness, (b) coast length and (c) velocity.

744 Figure 6: Additive models fitted to dispersal success (out-count) for 500 bootstrap samples of the  
745 coastal sites. (a) Proportion of deviance explained by the additive model for each larval duration.  
746 (b,c,d) Proportional loss of deviance explained when each term is dropped from the model, and total  
747 deviance explained by the model, for each larval duration. (e,f,g) Fitted parameter values for each  
748 term.

749 Figure 7: Additive models fitted to the number of arriving particles (in-count) at each site. (a)  
750 Proportion of deviance explained by the additive model for each larval duration. (b,c,d) Proportional  
751 loss of deviance explained when each term is dropped from the model, and total deviance explained  
752 by the model, for each larval duration. (e,f,g) Fitted parameter values for each term.

753 Figure 8: Summary statistics for particle tracking runs: (a) mean distance travelled by all particles,  
754 and (b) proportion of larvae dispersing successfully to a habitat site. Values are presented for  
755 June/October 2011 surface dwelling particles (thick/thin solid line), and June/October 2011 vertically  
756 migrating particles (thick/thin dashed line).

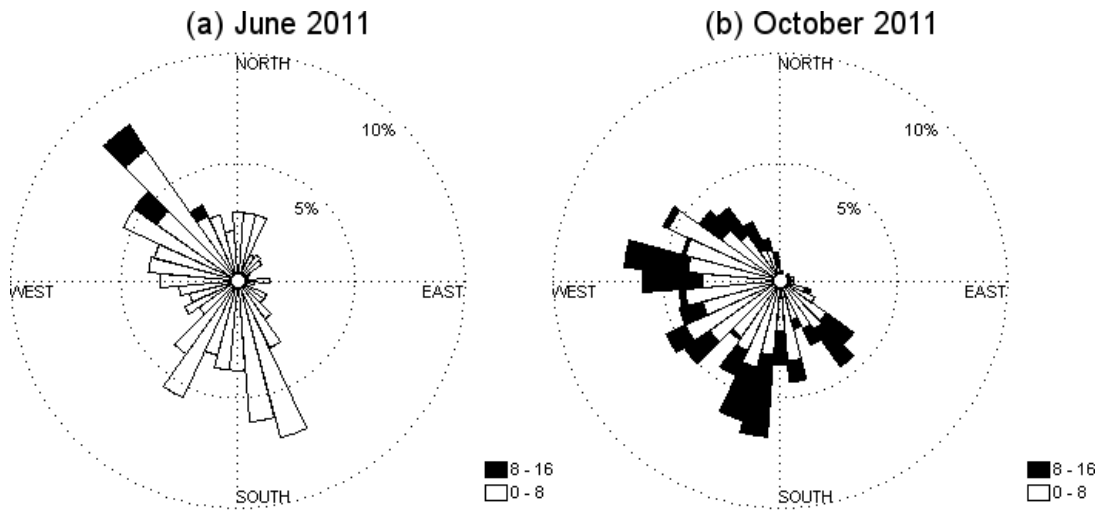
757 Figure 9: (a) Observed abundance of one of the most common species found in the region, the  
758 barnacle *Chthamalus montagui* L. Rare,  $<1\text{m}^{-2}$ ; Occasional,  $1-99\text{m}^{-2}$ ; Frequent,  $1-9$  per  $100\text{cm}^2$  ;  
759 Common,  $0.1-0.99\text{cm}^{-2}$ ; Abundant,  $1-3\text{cm}^{-2}$ ; Superabundant,  $>3\text{cm}^{-2}$ . Sites outside the model domain  
760 are shaded grey. (b) Relative value of the computed number of arrivals at all model habitat sites for  
761 16 day larval duration. (c) Comparison between observed abundance and model average number of  
762 arrivals within 10km radius of each observation site.



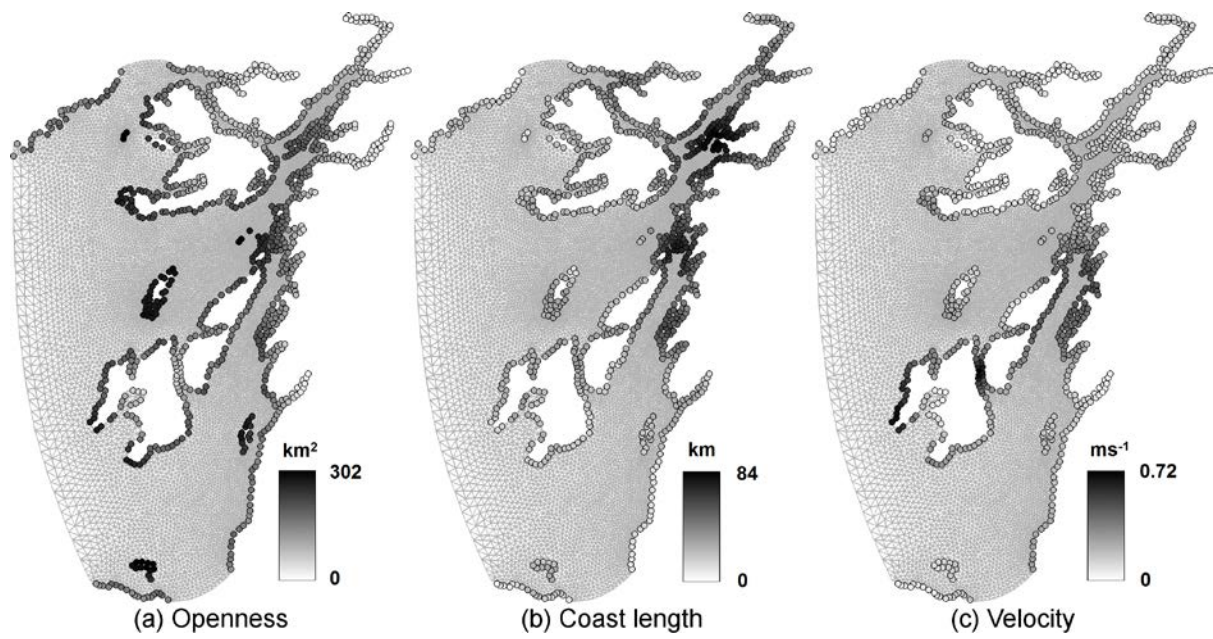
763

20km

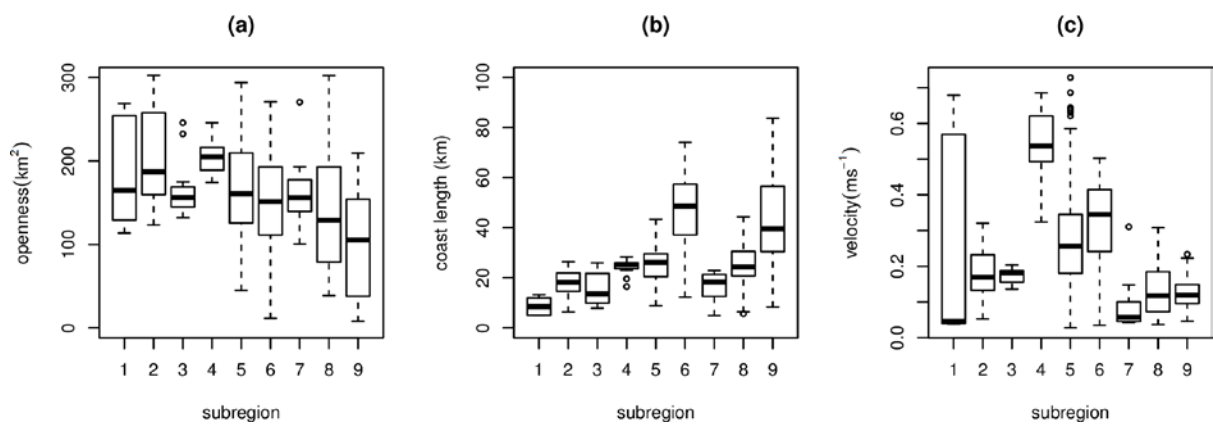
764



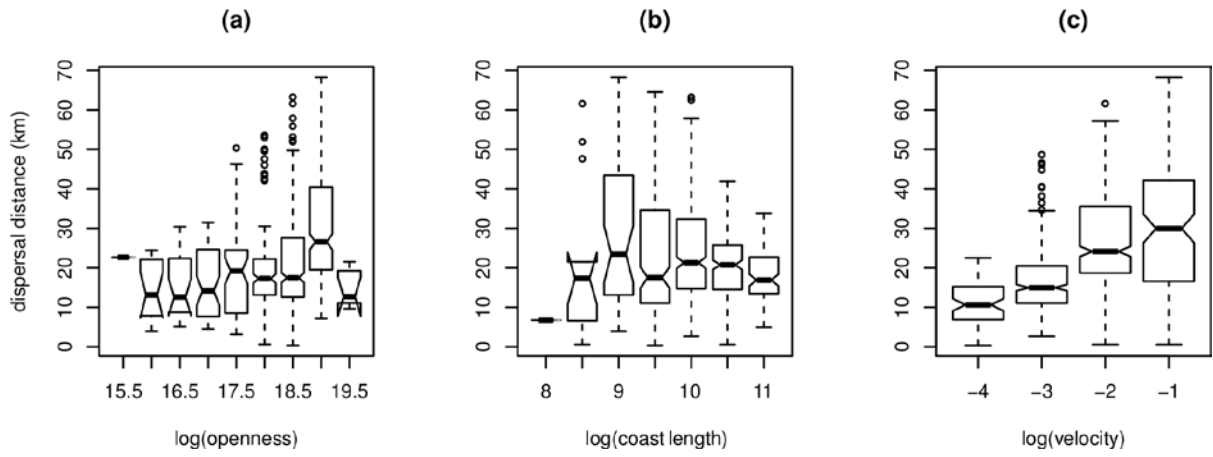
765 **Direction is FROM**



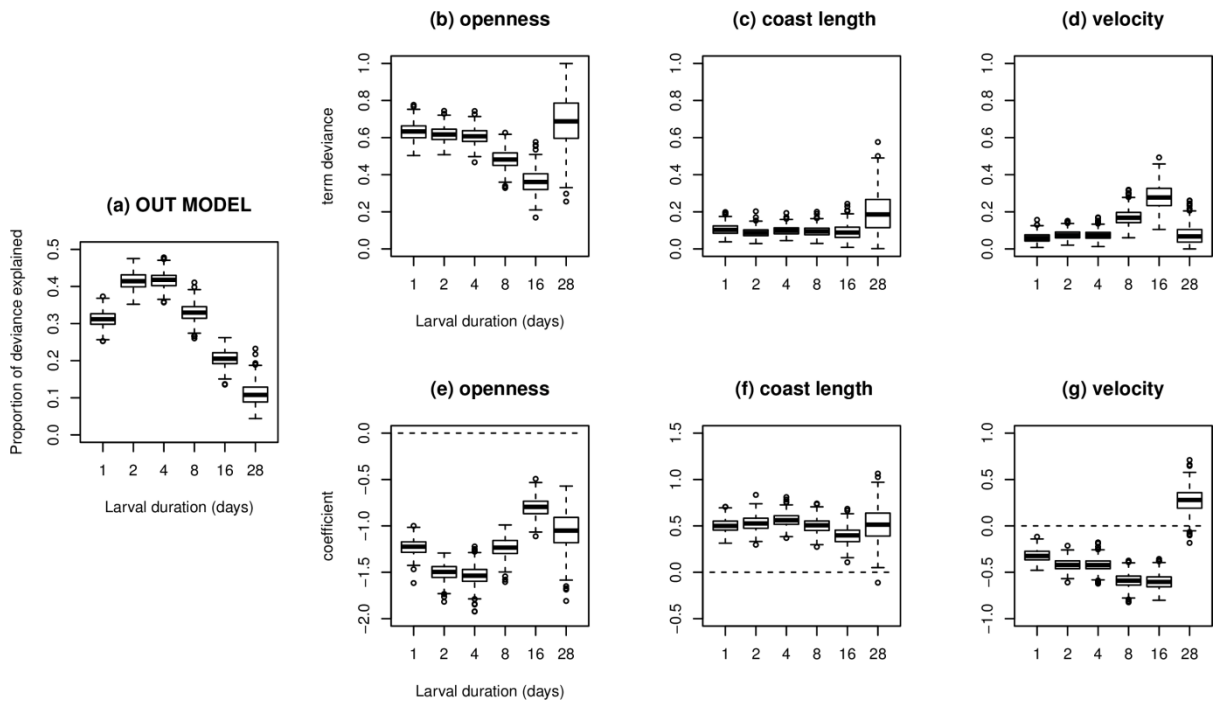
766



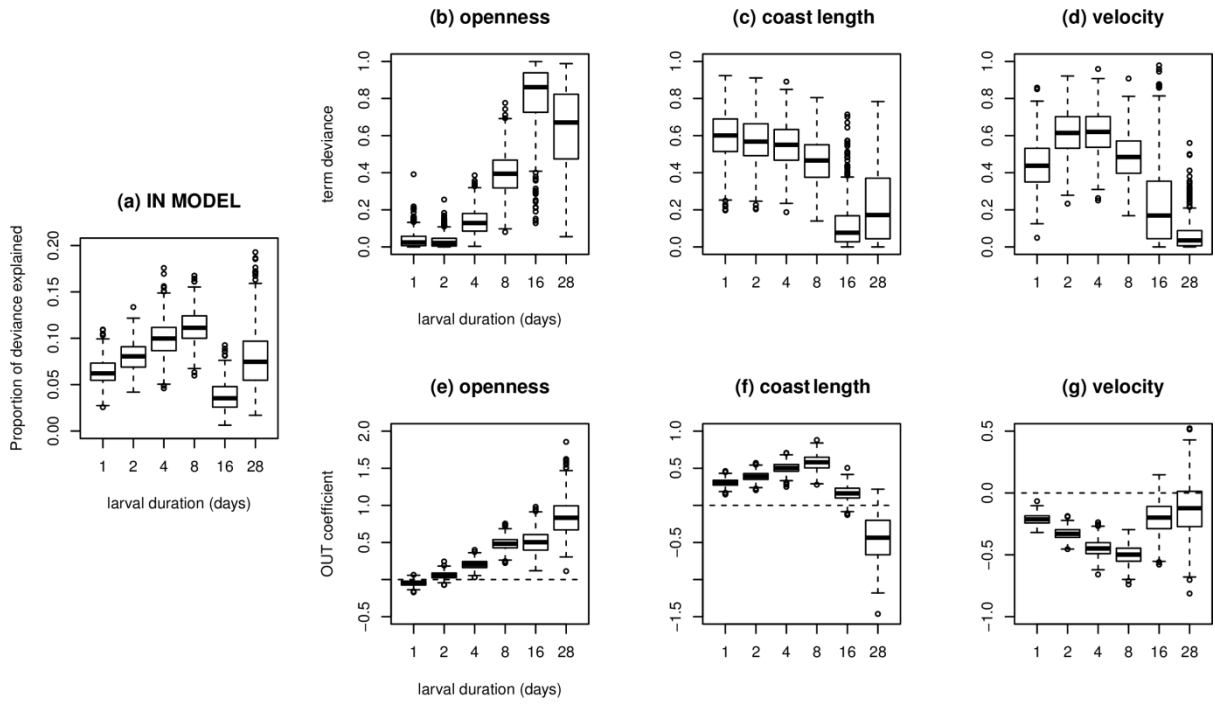
767



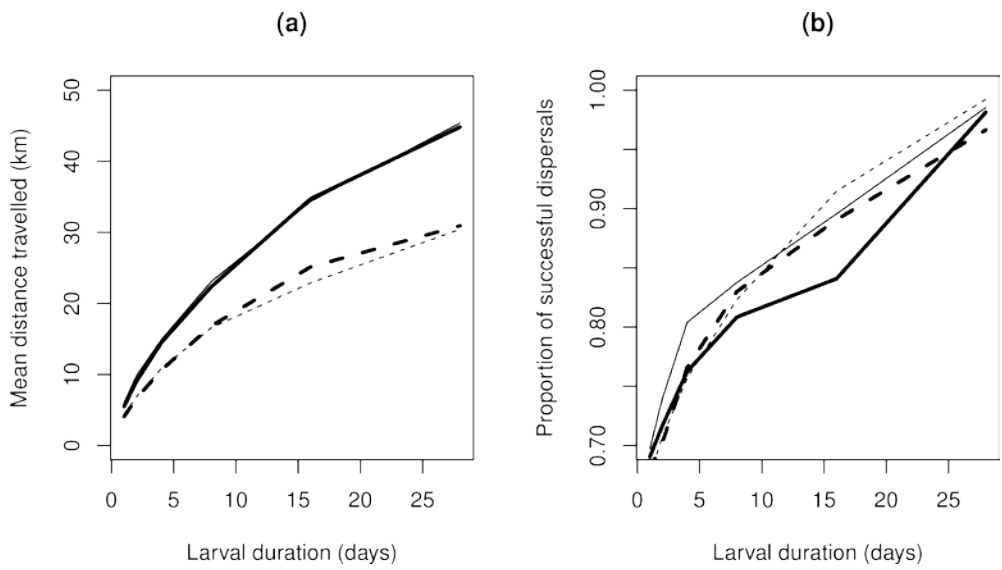
768



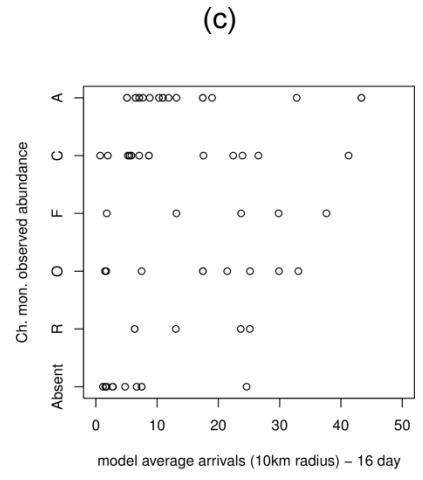
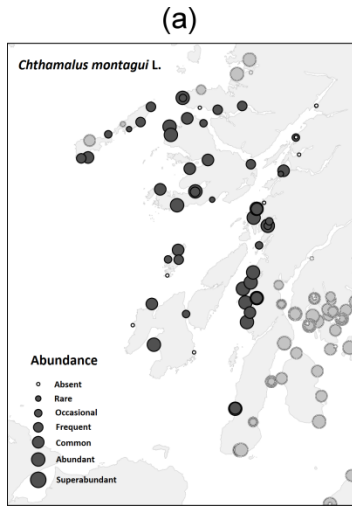
769



770



771





## Appendix 1: Hydrodynamic model detail

### 1.1 Unstructured model description

The ocean model for this study was based on the unstructured grid Finite Volume Coastal Ocean Model (FVCOM; Chen et al., 2003). The latest code (FVCOM 3.1.6) implementation includes advantages of both finite-element methods for geometric flexibility and finite-difference methods for discrete computation in effective MPI parallelized environments. Vertically, we used 11 terrain-following sigma-coordinates, which allows increased resolution in upper and bottom layers. In the horizontal the governing equations were discretized on a non-overlapped specially varying triangular mesh (25071 triangles, 14000 nodes), fitted to the irregular coastal geometry of south-west Scotland. This was refined over steep glacially over-deepened bathymetric features and around islands and narrow straits.

Model bathymetry was based on a combination of gridded SeaZone database (EDINA Digimap 2007), high resolution Admiralty charts and recent side-sonar and multibeam surveys undertaken by SAMS between 1999-2012 (J. Howe, unpublished data). Shallow areas with depth less than 10 m occupy 8% of the domain area and less than 1.4% of its volume, and so the minimum model depth was set to 10 m. For computational efficiency the capability for wetting and drying was not applied. To avoid the hydrostatic inconsistency problem typical of sigma-coordinate ocean models a procedure of overall volume-preserving bathymetric smoothing was applied, similar to Foreman et al., 2009). We set a restriction on the slope ratio  $r_h = \Delta h / \Delta L$ , where  $\Delta h$  is maximal depth difference, and  $\Delta L$  is horizontal side length, within each mesh triangle at  $r_h = 0.3$ .

The momentum flux through the sides of each triangle/prism discretization was based on the finite-volume method and calculated with the second-order accurate scheme (Kobayashi et al., 1999). Volume flux for scalars (temperature, salinity) was performed along with vertical velocity adjustment, which was required for the exact scalar quantity conservation. Horizontal diffusion in the model was based on the Smagorinsky (1963) eddy parameterisation, with mixing coefficient  $C=0.2$ . For turbulent vertical mixing parameterisation, and calculations of vertical eddy diffusivity  $K_m$  and vertical thermal diffusion  $K_h$ , we used the Mellor-Yamada 2.5 level turbulence closure model (Mellor and Yamada, 1982) with molecular kinetic diffusion  $\nu=1 \cdot 10^{-5}$  as the background value.

Existing bottom visual data in narrow straits and near shore rocks shows presence of strong near-bottom current capable of moving stones with settled seaweeds, while in several inner basins (e.g. Loch Etive) mud surfaces are nearly undisturbed, confirming high variability in bottom roughness

parameters. Bottom drag coefficient  $C_d$  was defined in the model with logarithmic-law  $C_d = \max\{\kappa^2 / \ln[(Z / Z_0)^2], C_{d0}\}$ , with von Karman constant  $\kappa=0.4$ , and  $Z$  the vertical distance from the bottom to the nearest velocity grid point. Since spatial variation of the bottom roughness parameters is not directly determined, we chose to globally assign the minimal constant values  $C_{d0}=0.0025$  and parameter  $Z_0=0.003$ .

The model was designed in Cartesian coordinates and solved numerically with a mode-split integration method. For the selected mesh geometry (edge length varies between 70 and 4650 m), the upper bound of the shortest external (barotropic) time step was defined as  $\Delta T_E=0.47$  seconds. The actual value implemented was 0.4s, to allow for the propagation of surface waves associated with sporadic strong tunnelling winds. The internal (baroclinic) mode time step (4s) was defined as  $\Delta T_I = I_{split} \Delta T_E$ , where  $I_{split}=10$ . Model integration time for a 5 month run was 24 hours, using 192 AMD Interlagos Opteron 2.3 GHz processors. Similar models have also been applied to the Loch Eive and Loch Fyne domains.

## 1.2 Model forcing

The model's initial temperature and salinity field was constructed by combining data from the climatological  $0.25^\circ$  grid provided by UK Hydrographic Office and irregular local CTD data sets. This was resampled on the triangular mesh using a distance weighted algorithm (Barnes 1964). The model develops a full-domain T, S field adjustment to the tidally forced current field within a fortnightly spin-up period.

Meteo-forcing for the FVCOM model includes precipitation and evaporation rates, atmospheric sea level pressure, east-west and north-south components of the winds at 10 m height, short wave radiation and net heat flux. Net heat flux was defined as a sum of short-wave, long-wave, sensible and latent heat fluxes. For calculation of the evaporation rate and heat fluxes we used standard bulk-formulae COARE algorithms (Fairall et al., 2003). Hourly data from 5 coastal Met-Office weather stations in the Argyll region, separated by distances of 15-50 km (Dunstaffnage, Tiree Airport, Machrihanish, Islay-Port-Ellen and Lochgilphead), were redistributed on a  $20 \times 20$  km grid over the model domain using a distance weighted algorithm (Barnes, 1964). Time series of daily fresh water discharge for the 28 main rivers in the area were constructed from watershed areas (1986), seasonally varying evapotranspiration factor (0.7-0.9), and daily estimates of precipitation rate converted from hourly data of the Met-Office weather stations. The water temperature at river mouths was defined as a combination of mean air and available mean sea-surface temperature, derived from Saulmore temperature loggers (M. Sayer, NERC Diving Unit) and sub-surface Access#11 thermistor chains (K. Jackson, SAMS).

Boundary conditions for the hydrodynamic model were derived from the 3-hourly output of the North East Atlantic Model, based on ROMS regular 2x2 km grid. This was developed by partners in EU FP7 ASIMUTH project at the Irish Marine Institute (<http://www.marine.ie>). Temperature, salinity, horizontal velocity components, 2-D fields of vertically averaged horizontal velocities and sea surface height were interpolated in 3D space to the 84 open boundary nodes/elements of the FVCOM domain. Initial experiments used tidal forcing provided by constructed tidal elevation timeseries. We introduced also a 6 km wide sponge layer to suppress noise along the model boundary. In the second series of experiments instead of tidal elevation time series we applied the tidal spectral data (amplitude and phase) using 11 tidal constituents (M2, S2, N2, K2, K1, O1, P1, Q1, M4, MS4, MN4) at the open boundary locations, derived from the 1/30° NW European shelf OSU Tidal Data Inversion model (Egbert et al., 2010). These compare more favourably with observed data, and are used in the results presented in this paper.

### **1.3 Model validation**

Model validation against available tidal information revealed similarity between the 5 month long model simulation results and well-known patterns in the distribution of the 4 main tidal constituents (M2, S2, K1 and O1), shown on admiralty charts and in literature (Jones, J. and Davies, A. 2005). Semidiurnal signal dominates in the area and the M2 amplitude increases from 0.4 m south of Islay to 1.1 m in the Tiree Passage as shown on the computed co-tidal chart (Figure A1). The model also correctly locates the M2 tidal amphidrome between Islay, Kintyre and N. Ireland. The model slightly underestimates the amplitudes of the main constituents (~10%), presumably because its open boundary forcing is derived from a model system (ROMS/Mercator) that relies on assimilated satellite altimetry data for sea surface topography, which commonly are not well resolved in close proximity to the coastline. Both long-term seasonal signal and short-term variability, when driven by regional weather undulations in heat flux and run-off, reproduce their essential effect on the hydro-physical characteristics of coastal waters in the area. These signals are well-represented in the modelled sea-water Salinity and Temperature fields. Comparisons between data from moorings deployed in two widely separated locations (the Tiree Passage, and the Hypox site in upper Loch Etive with brackish waters) and respective model predictions are shown on Figure A2.

## 1.4 References

- Barnes, S. L. 1964. A Technique for Maximising Details in Numerical Weather Map Analysis. *Journal of Applied Meteorology* 3: 369–409.
- Chen, C. et al. 2003. An Unstructured Grid, Finite-Volume, Three-Dimensional, Primitive Equations Ocean Model: Application to Coastal Ocean and Estuaries. *Journal of Atmospheric and Oceanic Technology* 20: 159–186.
- Egbert, G. D. et al. 2010. Assimilation of altimetry data for nonlinear shallow-water tides: Quarter-diurnal tides of the Northwest European Shelf. *Continental Shelf Research* 30: 668–679.
- Fairall, C. W. et al. 2003. Bulk Parameterization of Air–Sea Fluxes: Updates and Verification for the COARE Algorithm. *Journal of Climate* 16: 571–591.
- Foreman, M. G. G. et al. 2009. A finite volume model simulation for the Broughton Archipelago, Canada. *Ocean Modelling* 30: 29–47.
- Jones, J. and Davies, A. 2005. An intercomparison between finite difference and finite element (TELEMAC) approaches to modelling west coast of Britain tides. *Ocean Dynamics* 55: 178–198.
- Kobayashi, M. H. et al. 1999. A Conservative Finite-Volume Second-Order-Accurate Projection Method on Hybrid Unstructured Grids. *Journal of Computational Physics* 150: 40–75.
- Mellor, G. and Yamada, T. 1982. Development of a turbulence closure model for geophysical fluid problems. *Reviews of Geophysics and Space Physics* 20: 851–875.
- Smagorinsky, J. 1963. General circulation experiments with the primitive equations. *Monthly Weather Review* 91: 99–164.

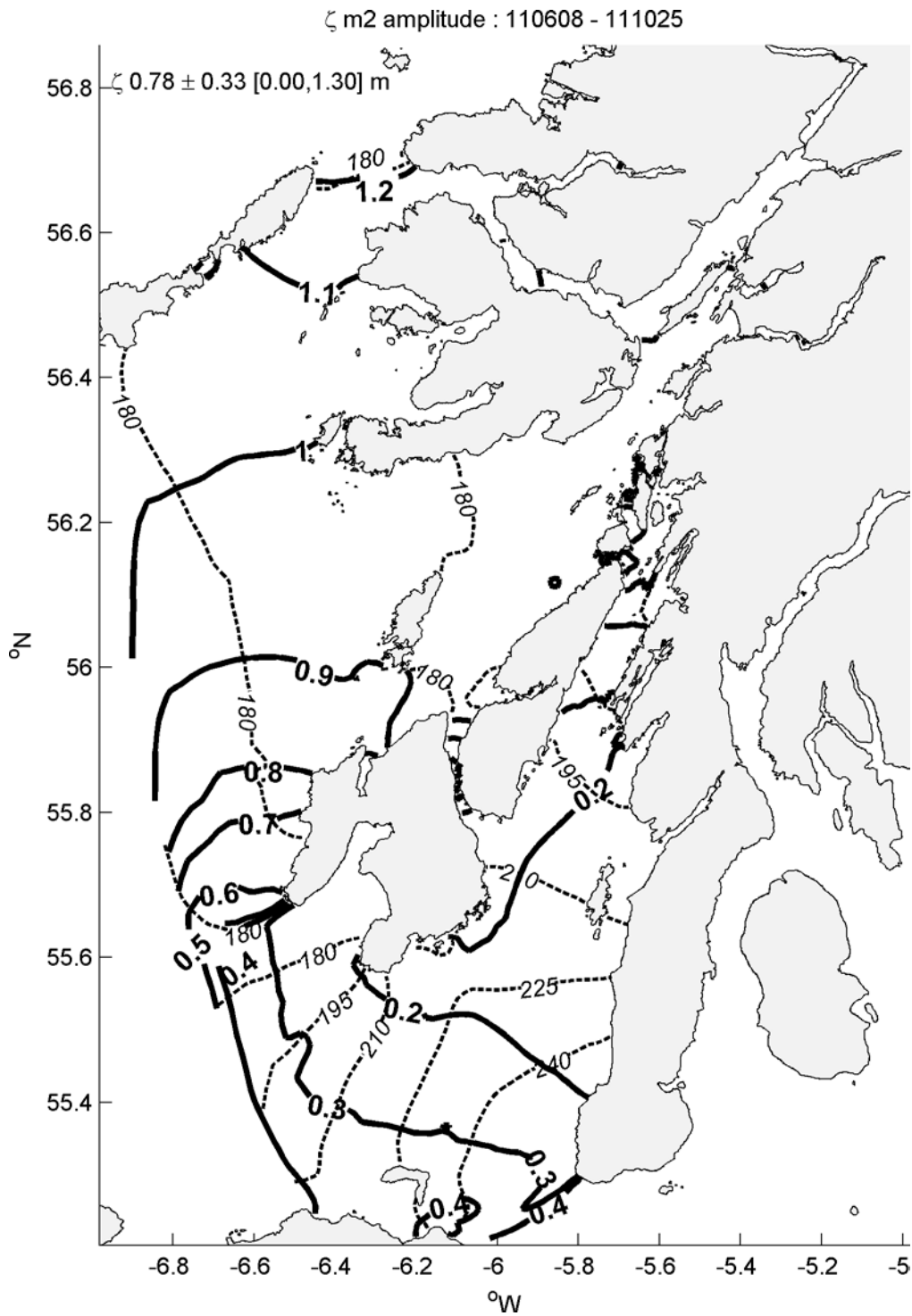


Figure A1: Co-tidal chart computed for M2 amplitude in meters (solid line) and phase in degrees (dashed lines).

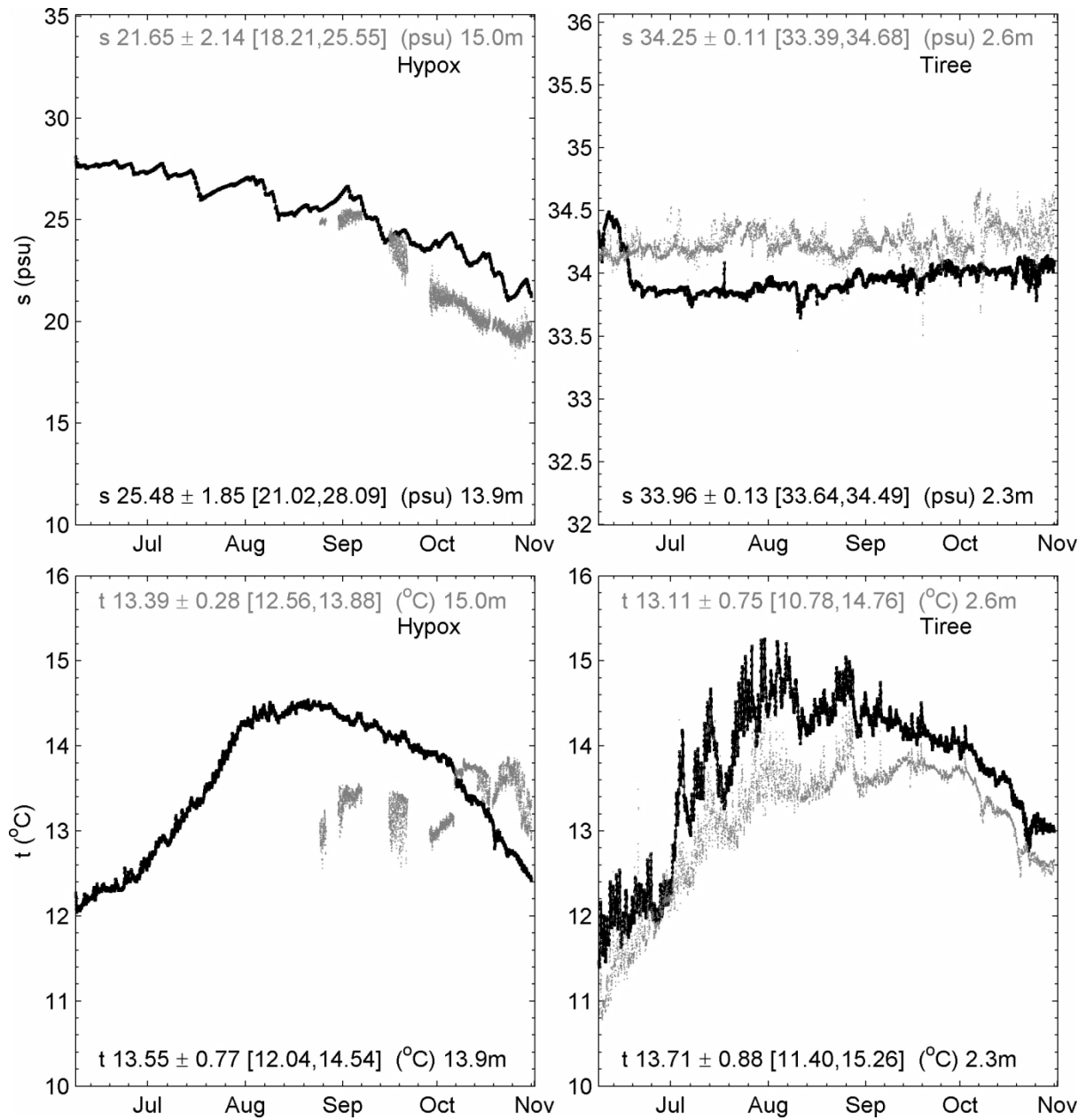


Figure A2: Comparison of the model (thick black line) and mooring (thin grey line) data. Salinity (upper panels) and Temperature (lower panels) at Hypox mooring in upper Loch Etive 56.458°N, 5.178°W (left) and in Tiree passage 56.63°N, 6.39°W (right). The data statistics (average, standard deviation, range and depth of measurement) are at the top of each panel, and equivalent model output statistics are at the base of each panel.

## Appendix 2: Particle tracking results - Supplementary figures

### 2.1 Main regression

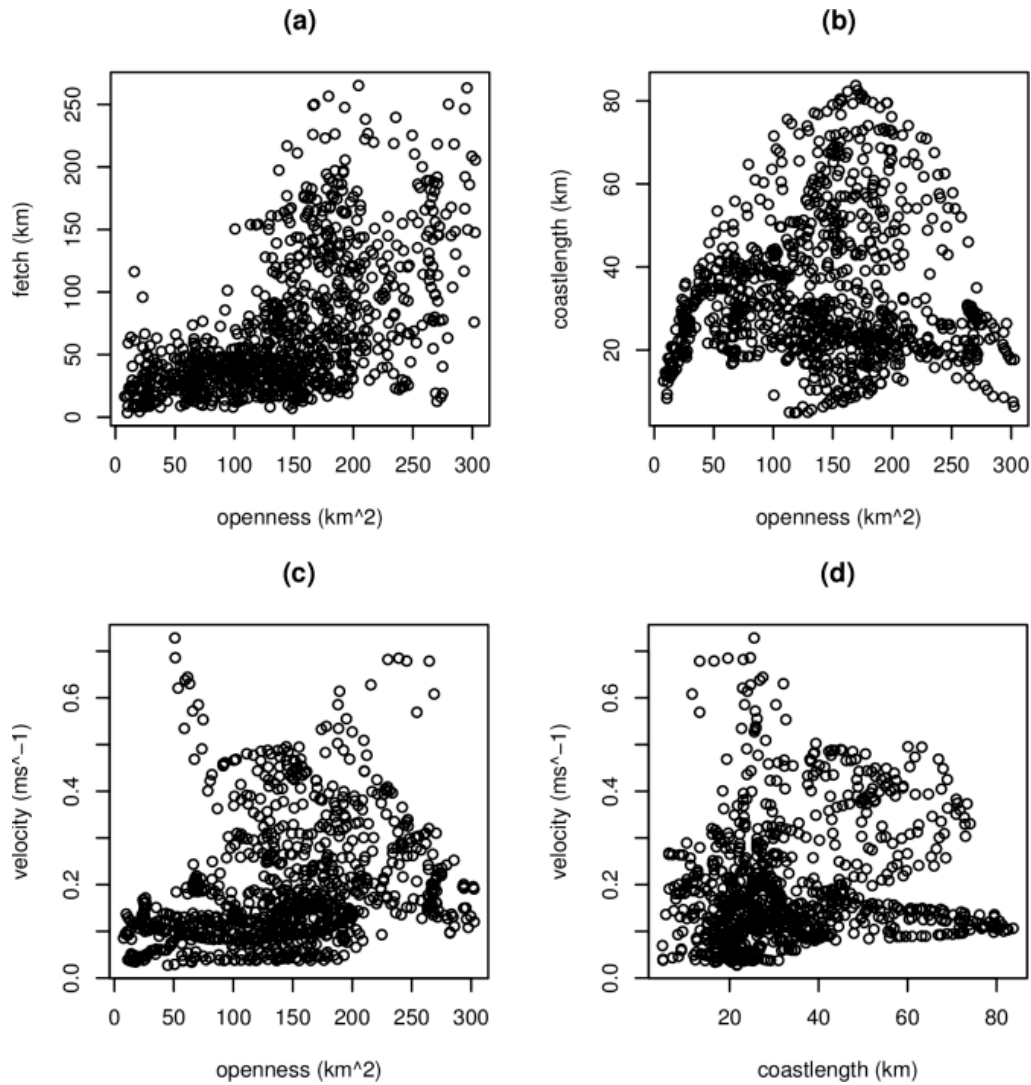
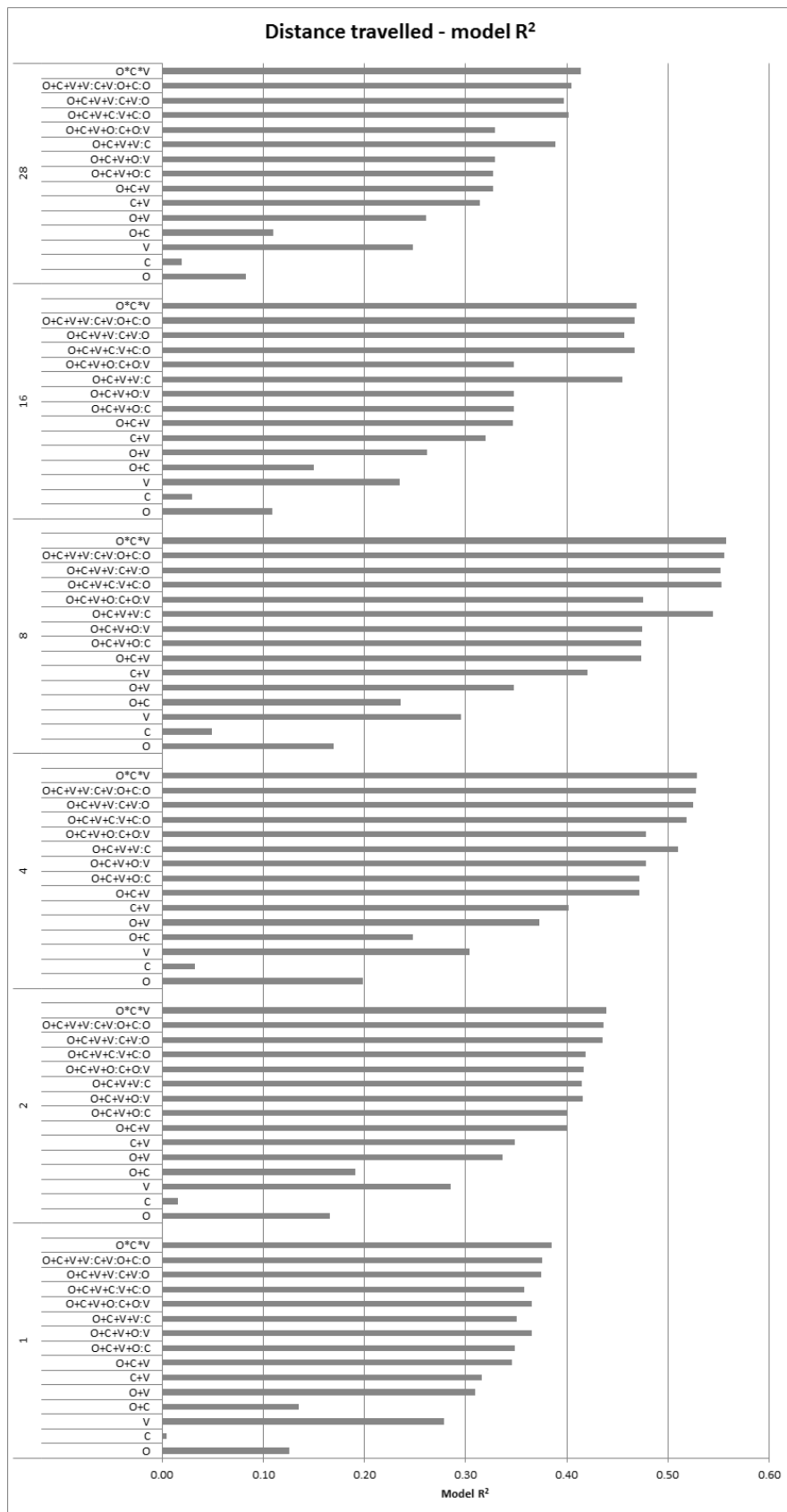
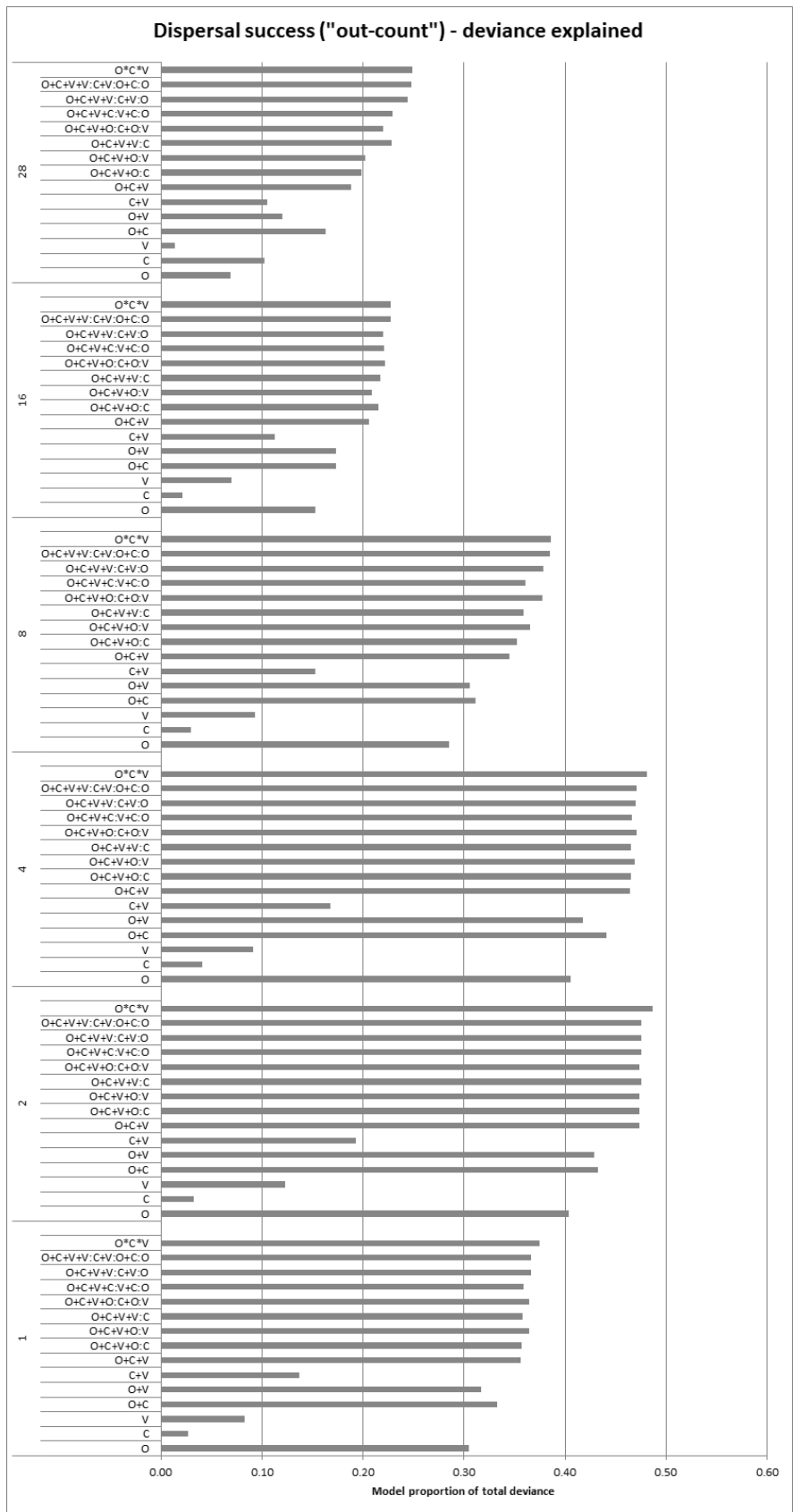


Figure A3: Metrics computed from the hydrodynamic model mesh, for each of the 940 coastal sites used as particle tracking habitat, plotted against one another. The strong relationship between fetch and openness meant that regression analysis omitted fetch.



**Figure A4: R<sup>2</sup> of linear regression models fitted to dispersal distance (June 2011, surface particles). Velocity is the most important variable, and alone accounts for a large portion of the variance explained by the more complicated models.**





**Figure A5: Proportion of deviance explained by binomial regression models fitted to site dispersal success (June 2011, surface particles). Openness is the most important variable, alone accounting for around 75-90% of the deviance explained by a complete interaction model at longer larval durations.**

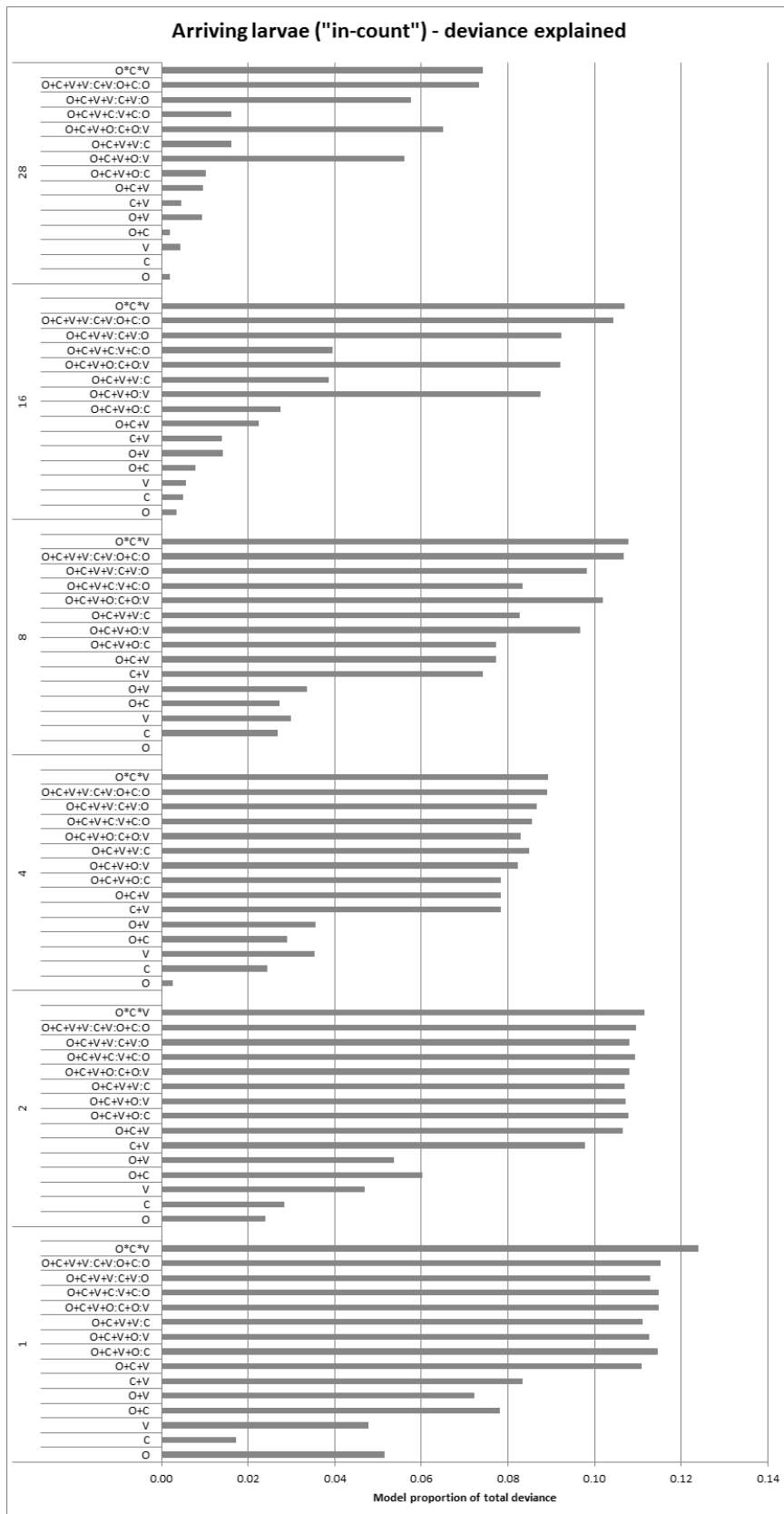


**Figure A6: Proportion of deviance explained by logistic regression models fitted to the number of arriving larvae (June 2011, surface particles). Models in general fare poorly, and individual terms do not account for large portions of the deviance. Additive models of coast length and velocity do fare quite well for short larval durations, but for longer durations interaction terms are necessary.**

## 2.2 Vertically migrating larvae

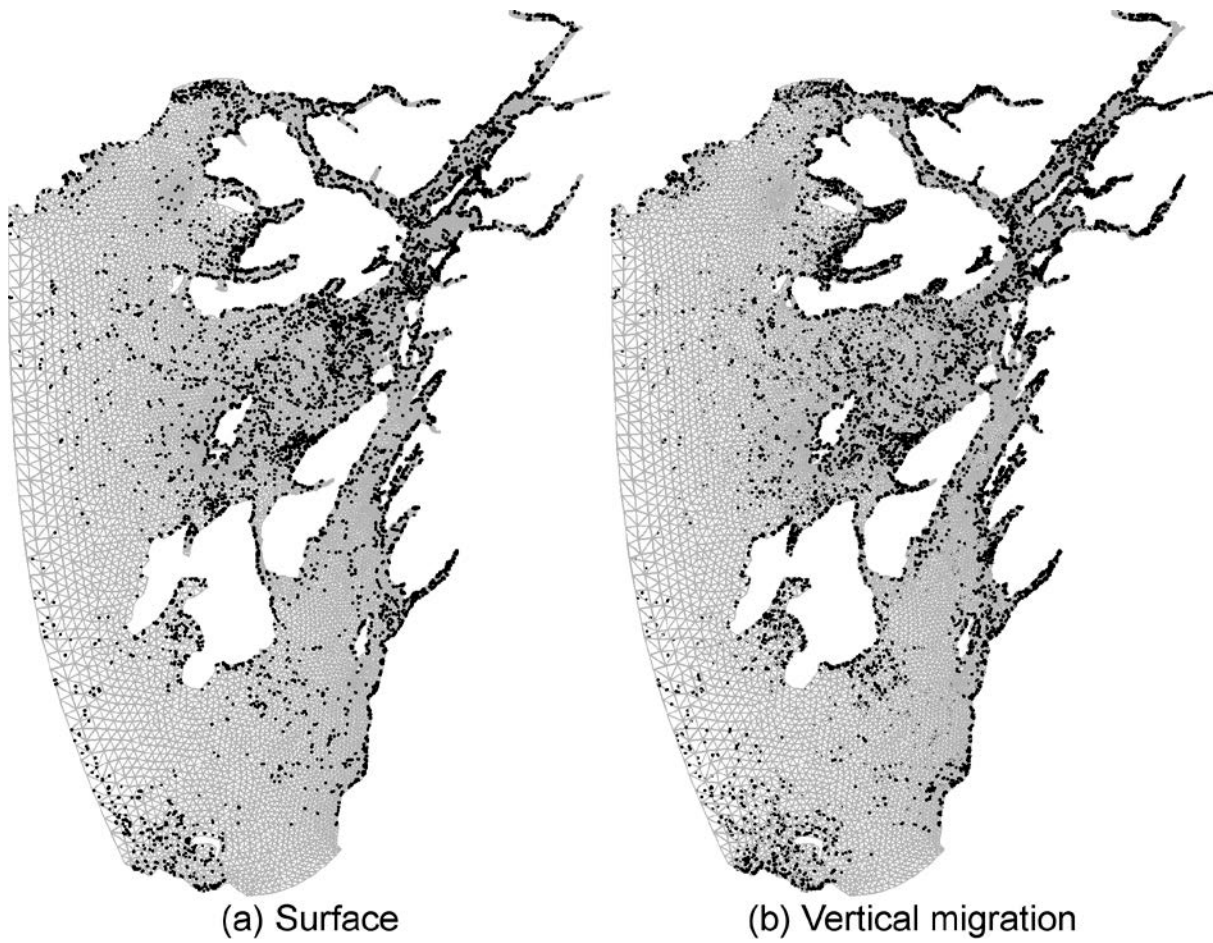
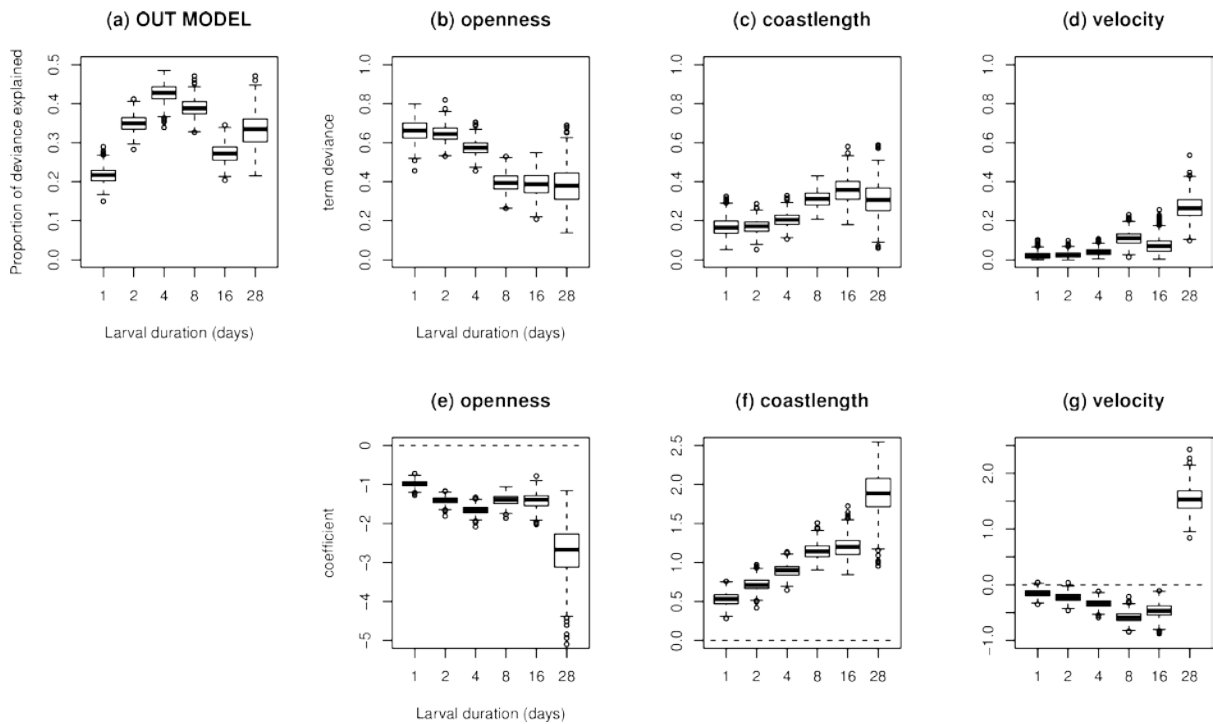
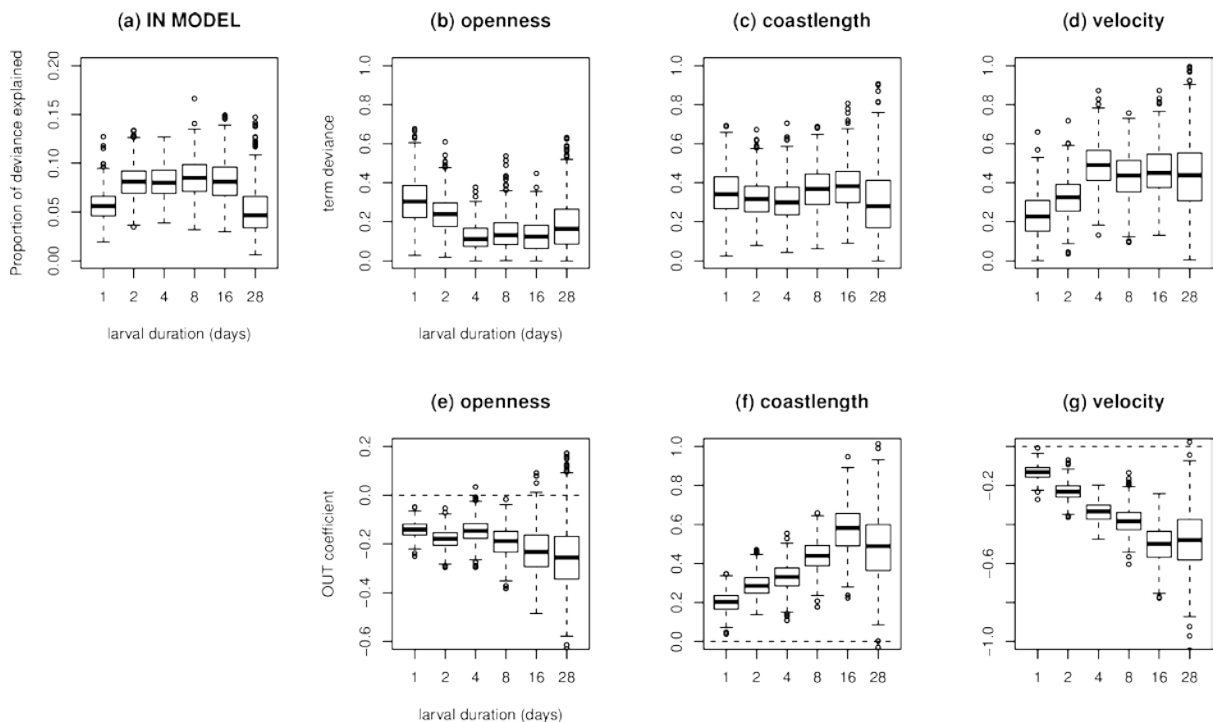


Figure A7: Final locations of larval particles with a 2 day duration: (a) surface dwelling particles only; and (b) Vertically migrating particles. The latter tend to be retained closer to the coastline.



**Figure A8: Additive models fitted to out-counts (number of successful dispersals) for particles that move to the surface during the flood tide, and the bed during the ebb. (a) Proportion of deviance explained by the additive model for each larval duration. (b,c,d) Proportional loss of deviance explained when each term is dropped from the model, and total deviance explained by the model, for each larval duration. (e,f,g) Fitted parameter values for each term.**



**Figure A9: Additive models fitted to in-counts (number arriving particles) for particles that move to the surface during the flood tide, and the bed during the ebb. (a) Proportion of deviance explained by the additive model for each larval duration. (b,c,d) Proportional loss of deviance explained when each term is dropped from the model, and total deviance explained by the model, for each larval duration. (e,f,g) Fitted parameter values for each term.**

## 2.3 October 2011

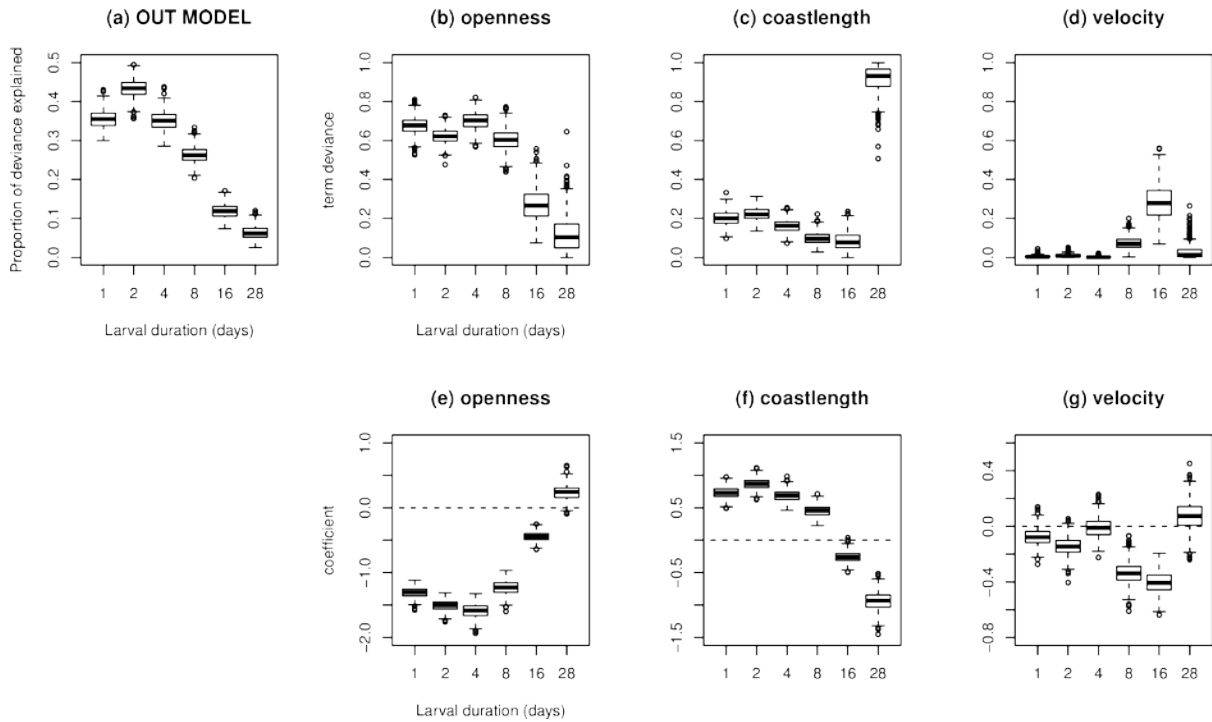


**Figure A10: October 2011. Additive models fitted to out-counts (number of successful dispersals). (a) Proportion of deviance explained by the additive model for each larval duration. (b,c,d) Proportional loss of deviance explained when each term is dropped from the model, and total deviance explained by the model, for each larval duration. (e,f,g) Fitted parameter values for each term.**

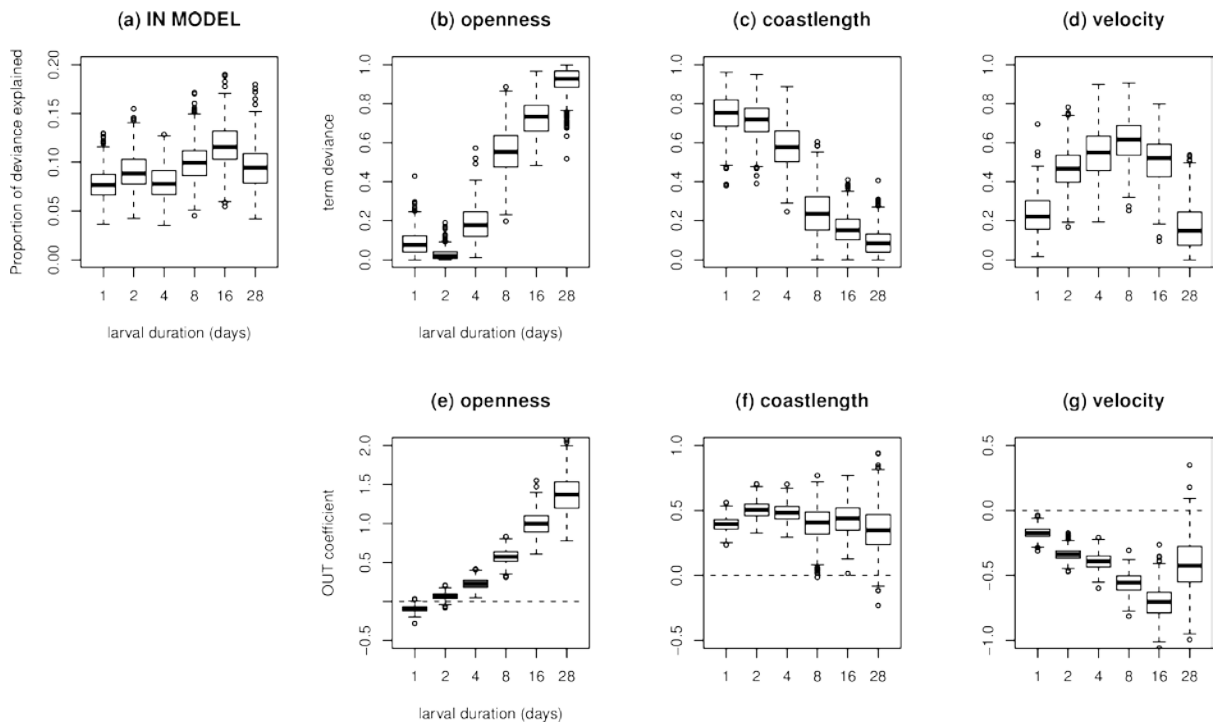


**Figure A11: October 2011. Additive models fitted to in-counts (number arriving particles). (a) Proportion of deviance explained by the additive model for each larval duration. (b,c,d) Proportional loss of deviance explained when each term is dropped from the model, and total deviance explained by the model, for each larval duration. (e,f,g) Fitted parameter values for each term.**

## 2.4 Spatial correlation of model residuals

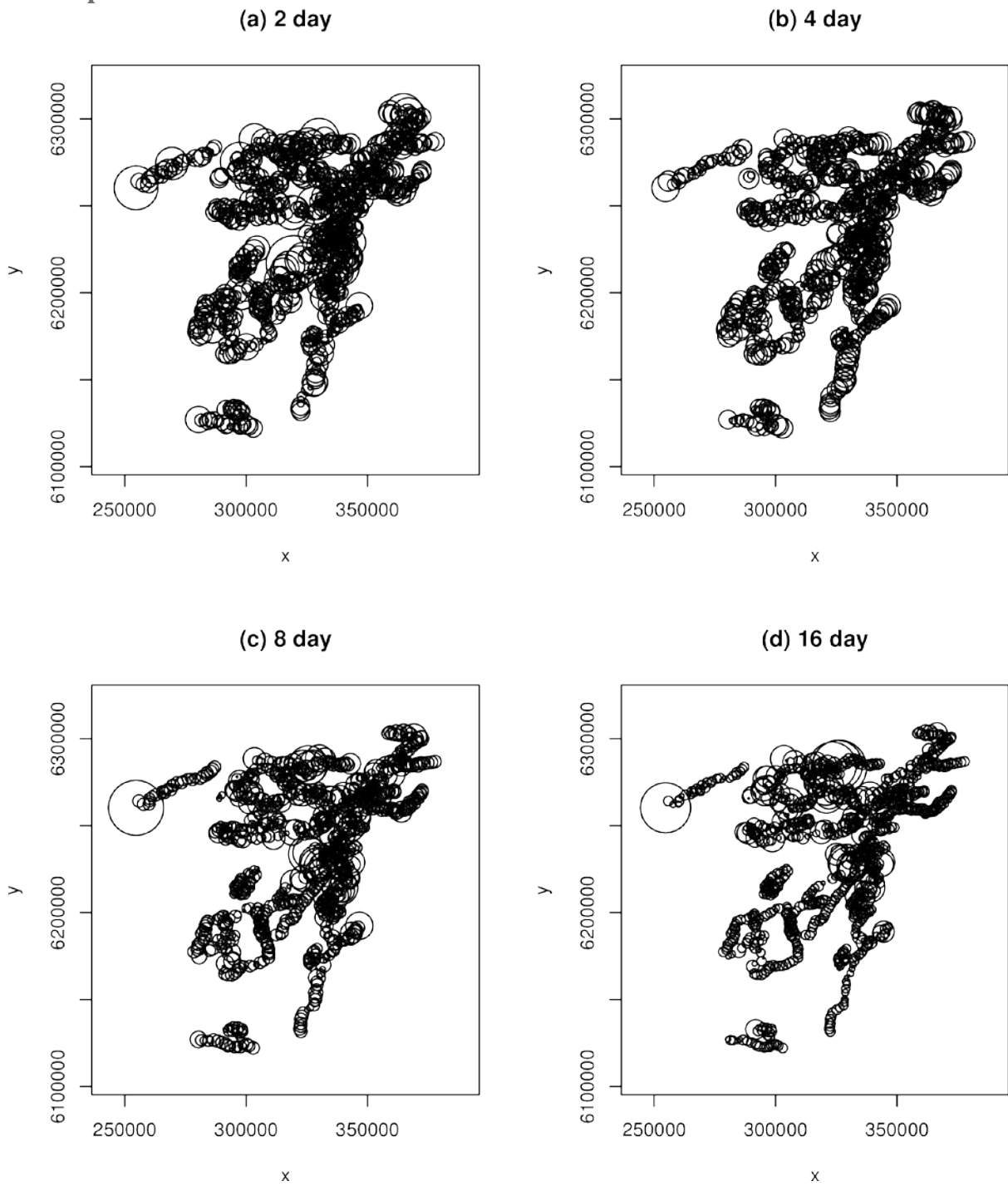
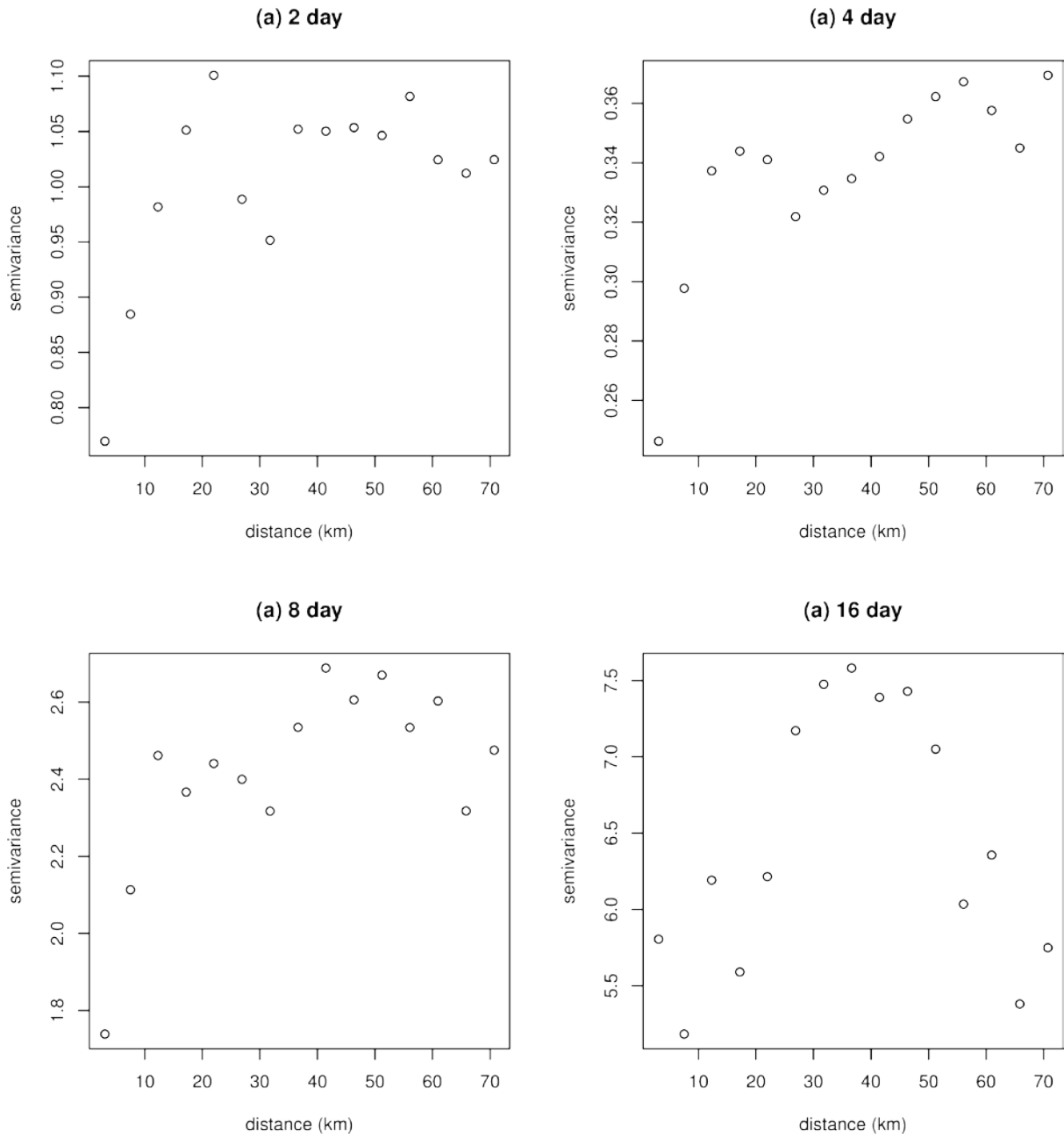


Figure A12: Maps of model residuals for single GLM fits to the number of arriving larvae for (a) 2, (b) 4, (c) 8 and (d) 16 day larval duration.



**Figure A13: Semivariograms for model residuals for single GLM fits to the number of arriving larvae over the entire domain. Residuals at small separations tend to be more similar than those at longer ranges, indicating the elevated number of arrivals observed in proximity to particular geographic features.**